H_2O IN RHYOLITIC GLASSES AND MELTS: MEASUREMENT, SPECIATION, SOLUBILITY, AND DIFFUSION

Youxue Zhang
Department of Geological Sciences
University of Michigan, Ann Arbor

Abstract. Dissolved H_2O in silicate melts and glasses plays a crucial role in volcanic eruptions on terrestrial planets and affects glass properties and magma evolution. In this paper, major progress on several aspects of the H_2O-melt (or glass) system is reviewed, consistency among a variety of data is investigated, discrepancies are evaluated, and confusion is clarified. On the infrared measurement of total H_2O and species concentrations, calibration for a variety of glasses has been carried out at room temperature. The measurements for H_2O in rhyolitic glasses have undergone the most scrutiny, resulting in the realization that absorptivities for the near-infrared bands depend on total H_2O content. Although the variation of the absorptivities does not seem to significantly affect the determination of total H_2O, it does affect the determination of molecular H_2O and OH species concentrations. Calibration of the infrared technique for H_2O in rhyolitic glasses still needs much improvement, especially at high total H_2O. Furthermore, it is now almost certain that the molar absorptivities also depend on the measurement temperature in in situ studies. Hence it will be necessary to carry out calibrations in situ at high temperatures. On H_2O speciation, results from two experimental approaches, the quench technique and the in situ technique, are very different, leading to controversy in our understanding of true speciation. A solution is presented to reconcile this controversy. It is almost certain that the quench technique does not suffer from a quench problem, but interpretation of in situ results suffered from ignoring the dependence of the molar absorptivities on measurement temperature. Accurate calibration at high temperatures is necessary for the quantitative application of the in situ technique to H_2O speciation in silicate melts and glasses. On H_2O solubility in silicate melts, recent experimental work has significantly expanded the T–P range of solubility measurements, and recent solubility models fill a gap for predicting solubility for a wide range of melt compositions. I present a solubility model for rhyolitic and quasi-rhyolitic melts over a wide range of T and P (500°–1350°C, 0–8 kbar) by incorporating the role of speciation. The solubility model is able to recover the experimental solubility data and has extrapolative value, although the partial molar volume of H_2O derived from the solubility model differs from that derived from density measurements. On H_2O diffusion, recent studies on H_2O diffusion in a quasi-rhyolitic melt at 800°–1200°C, 0.5–5 kbar, and up to 7% total H_2O not only provide important new diffusion data, but are also challenging earlier understanding of H_2O diffusion based on data in rhyolitic glasses at 400°–550°C, 1 bar, and 0.2–1.8% total H_2O. A comparison between the earlier model and recent data is made. The recent high-temperature diffusivities at total $H_2O \leq 2\%$ can be predicted by the earlier model. However, at higher total H_2O, the earlier model fails. New work is under way to understand the diffusion mechanisms at high H_2O contents.

1. INTRODUCTION AND OVERVIEW

As the most abundant volatile component in terrestrial magmas, dissolved H_2O in magmas controls the eruptive power of magma on terrestrial planets [e.g., *Wilson*, 1980; *Wilson et al*., 1980; *Kieffer*, 1995]. The exsolution of dissolved H_2O from magmas most likely provided surface water on the terrestrial planets and hydrothermal fluids for ore formation. Dissolved H_2O in glasses affects glass properties. Dissolved H_2O in silicate melt affects its properties and evolution, such as viscosity [e.g., *Shaw*, 1963, 1972; *Burnham*, 1967; *Stolper*, 1982a, b; *Schulze et al*., 1996; *Hess and Dingwell*, 1996], density [e.g., *Ochs and Lange*, 1997, 1999], diffusivity [e.g., *Watson*, 1979], liquidus and solidus temperatures [e.g., *Wasserburg*, 1957; *Tuttle and Bowen*, 1958; *Kushiro*, 1969; *Luth*, 1976; *Wyllie*, 1979], crystallization sequence [e.g., *Hamilton et al*., 1964; *Wyllie*, 1979; *Moore and Carmichael*, 1998], and crystal nucleation and growth [*Fenn*, 1977]. The special volume published by the Mineralogical Society of America [*Carroll and Holloway*, 1994] reviewed water (and other volatiles) in silicate melts and glasse. Chapters included contributions by *Ihinger et al*. [1994], *Burnham* [1994], *McMillan* [1994], *Johnson et al*. [1994], *Lange* [1994], and *Watson* [1994]. Many papers have been published on the subject since then. Although much progress has been made, controversies and confusion are abundant. In this paper I critically review work

Reviews of Geophysics, 37, 4 / *November 1999*
pages 493–516
8755-1209/99/1999RG900012*$15.00*
Paper number 1999RG900012

TABLE 1. Anhydrous Compositions of Some Glasses (wt %)

Sample	*SiO_2*	*TiO_2*	*Al_2O_3*	*FeO*	*MgO*	*CaO*	*Na_2O*	*K_2O*	*Sum*
Rhyolite[a]	76.59	0.08	12.67	1.00	0.03	0.52	3.98	4.88	99.75
2σ variation	0.55	0.09	0.16	0.18	0.03	0.05	0.26	0.39	
AOQ[b]	76.14	···	13.53	···	···	···	4.65	5.68	100.00
Shen and Keppler [1995][c]	82.5	···	11.6	···	···	···	5.2	···	99.3

[a]From *Zhang et al*. [1997a]. A variety of rhyolitic samples, all with similar composition, have been used to study solubility and viscosity of hydrous rhyolite [*Shaw*, 1963, 1974; *Silver et al*., 1990; *Ihinger*, 1991], to calibrate the infrared technique [*Newman et al*., 1986; *Ihinger et al*., 1994; *Zhang et al*., 1997a], to examine the temperature dependence of speciation [*Zhang et al*., 1991a; *Ihinger*, 1991; *Ihinger et al*., 1999], to examine the reaction kinetics of the speciation reaction [*Zhang et al*., 1991a, 1995, 1997b], and to investigate water diffusion [*Shaw*, 1974; *Zhang et al*., 1991a].

[b]This sample has a nominal composition of Qz28Ab38Or34 (where Qz means quartz, Ab means albite, and Or means orthoclase, $KAlSi_3O_8$) and has been used to investigate the temperature dependence of H_2O solubility [*Holtz et al*., 1992, 1995], to examine the temperature dependence of speciation (H_2O_t = 4.14%) in an in situ study [*Nowak and Behrens*, 1995], and to study H_2O diffusion [*Nowak and Behrens*, 1997].

[c]*Shen and Keppler* [1995] used this sample to examine the temperature dependence of speciation (H_2O_t = 8.1%) in an in situ study.

in the last 5 years on the dissolved H_2O component in rhyolitic melt/glass (a rhyolite is a fine-grained silicic igneous rock; see Table 1 for composition) and a quasi-rhyolitic composition (sample name AOQ; see Table 1), concentrating on clarification of controversies, assessment of data, and consistency of models.

1.1. H_2O Concentration and Speciation

H_2O_t content (hereinafter H_2O_t refers to total H_2O contents and H_2O refers to H_2O as a chemical component) in glasses can be determined by several techniques, including manometry, Karl-Fischer titration, infrared spectroscopy, and ion microprobe. H_2O_t content in natural silicate melts spans a large range. It is typically 0.2–0.4 wt % (hereinafter % refers to weight percent unless otherwise specified such as % relative, or mol %) in mid-ocean ridge basaltic glasses [e.g., *Dixon et al*., 1988] and 0.2–0.7% in Hawaiian basaltic glasses [e.g., *Dixon et al*., 1991]. Rhyolitic glasses in lava domes and flows often contain 0.08–0.8% H_2O_t, and those in pyroclastic deposits contain 0.6–3.0% H_2O_t [e.g., *Newman et al*., 1986; *Zhang et al*., 1991a, 1997a, b]. Glass inclusions in crystals may contain up to 7% H_2O_t [*Anderson et al*., 1989; *Skirius et al*., 1990; *Qin*, 1994; *Johnson et al*., 1994; *Wallace et al*., 1995; *Zhang et al*., 1997a]. Tektite glasses contain 0.01–0.1% H_2O_t [*Gilchrist et al*., 1969]. The H_2O_t content in primitive lunar glasses is often below detection limit (<50 ppm H_2O_t) [*Fogel and Rutherford*, 1995]. Although the H_2O_t contents of volcanic rocks on Venus and Mars are not known, occurrences of caldera-like structures suggest that the preeruptive H_2O_t contents in volcanic rocks may reach a few weight percent [e.g., *Kieffer*, 1995].

Infrared spectroscopy can be used to distinguish H_2O species in silicate glasses. A dissolved H_2O component is present in silicate melts and glasses in at least two species with distinct infrared bands [*Scholze*, 1960; *Stolper*, 1982a]: H_2O molecules (hereinafter referred to as H_2O_m) characterized by the near-infrared combination band at 5230 cm^{-1} (wavelength 1.91 μm; cm^{-1} is used for wavenumber unit, both to follow convention and to distinguish it from the thickness unit mm), and OH groups (OH means XOH, where X may be Si, Al, Na, etc., but not H) characterized by the combination band at 4520 cm^{-1} (2.21 μm) (Figure 1). The 5230 cm^{-1} band is a combination band due to HOH bending + OH basic stretching, and the 4520 cm^{-1} band is due to XOH bending/stretching + OH basic stretching [*Scholze*, 1960; *Stolper*, 1982a]. *Davis and Tomozawa* [1996] provided a comprehensive discussion of band assignment in hydrous silica glass. The reaction of dissolved H_2O_m with the network to form OH groups not only increases the solubility of H_2O, but also modifies the silicate network and depolymerizes the melt, accounting for the large effect of dissolved H_2O on melt properties.

1.2. Definitions of H_2O Mole Fractions

There are three definitions of H_2O mole fractions often encountered in literature, which may be somewhat confusing to nonspecialists. They are summarized below.

1. In the present work, mole fractions on a single-oxygen basis are used, following the work of *Stolper* [1982b]. The calculation of the mole fractions of H_2O_t, H_2O_m, OH, and O for hydrous rhyolitic melts/glasses is as follows:

$$[H_2O_t] = (C/18.015)/\{C/18.015 + (1 - C)/W\},$$

$$[H_2O_m] = [H_2O_t](H_2O_m)/(H_2O_t),$$

$$[OH] = 2\{[H_2O_t] - [H_2O_m]\},$$

$$[O] = 1 - [H_2O_m] - [OH],$$

where parentheses indicate mass fraction, C is the mass fraction of H_2O_t, and W is the mass of dry rhyolite (Table 1) per mole of oxygen and is 32.49 g/mol. For AOQ (a quasi-rhyolitic glass; Table 1) composition, W = 32.6 g/mol. For albite ($NaAlSi_3O_8$), W = 32.778 g/mol.

2. In the H_2O-$NaAlSi_3O_8$ system, *Burnham* [1975] and other authors following him treated $NaAlSi_3O_8$ as one unit (whereas the definition on a single oxygen basis treats $NaAlSi_3O_8$ as eight units). In this definition,

$X_{H_2O_t} = (C/18.015)/\{C/18.015 + (1 - C)/262.22\}$, where 262.22 is the molar mass of $NaAlSi_3O_8$.

3. Some authors [e.g., *Moore et al.*, 1998] defined the H_2O oxide mole fraction by treating each oxide (e.g., SiO_2) as one unit (whereas the definition on a single-oxygen basis treats SiO_2 as two units and treats Al_2O_3 as three units). In this definition, $X_{H_2O_t} = (C/18.015)/\Sigma(C_i/W_i)$, where C_i is the mass fraction of the oxide component i (including H_2O) and W_i is the molar mass of the oxide.

The above three different definitions result in very different mole fractions. For example, 5.0 wt % H_2O_t in albite melt translates into an H_2O_t mole fraction of 0.0874 on a single-oxygen basis, to 0.161 using oxide moles, and to 0.434 using $NaAlSi_3O_8$ as one unit.

The definition of mass fraction (or weight percent) of OH may also cause confusion. It does not mean the actual mass fraction of OH per se, but rather the mass fraction of extracted H_2O that was present in the glass as OH (or in the form of OH). That is, it is the mass fraction of the species 2OH − O (two OH groups minus one oxygen). In this way, in terms of mass fraction or weight percent, $(H_2O_t) = (H_2O_m) + (OH)$. The definition of mole fraction of OH, however, is the mole fraction of OH per se, not the mole fraction of 2OH − O. In terms of mole fraction, $[H_2O_t] = [H_2O_m] + [OH]/2$.

1.3. Reactions of H_2O With Melt, Equilibrium, and Kinetics

For an understanding of H_2O solubility in and interaction with a silicate melt, the equilibrium of two reactions needs to be considered. The first is the heterogeneous reaction between the melt and vapor phases:

$$\text{(R1)} \qquad H_2O\ (\text{vapor}) \Leftrightarrow H_2O_m\ (\text{melt}).$$

The equilibrium constant of the above reaction is

$$K_1 = \frac{[H_2O_m]}{f_{H_2O}}, \tag{1}$$

where the brackets refer to mole fraction in the melt/glass phase on a single-oxygen basis. Since mole fraction instead of activity is used in the above equation, K_1 is not an equilibrium constant in the strict sense and may depend on H_2O_t. However, activities are difficult to determine. *Zhang et al.* [1997a] have found that dissolved H_2O_m and OH behave roughly ideally at least up to 2.4% H_2O_t based on species equilibrium data. Hence the mole fraction of H_2O_m approximates the activity of H_2O_m, which is also the activity of the H_2O component in silicate melt. K_1 is hence used as the proxy for the equilibrium constant.

The second reaction is the homogeneous reaction in the silicate melt/glass phase for species interconversion:

$$\text{(R2)} \quad H_2O_m\ (\text{melt}) + O\ (\text{melt}) \Leftrightarrow 2OH\ (\text{melt}),$$

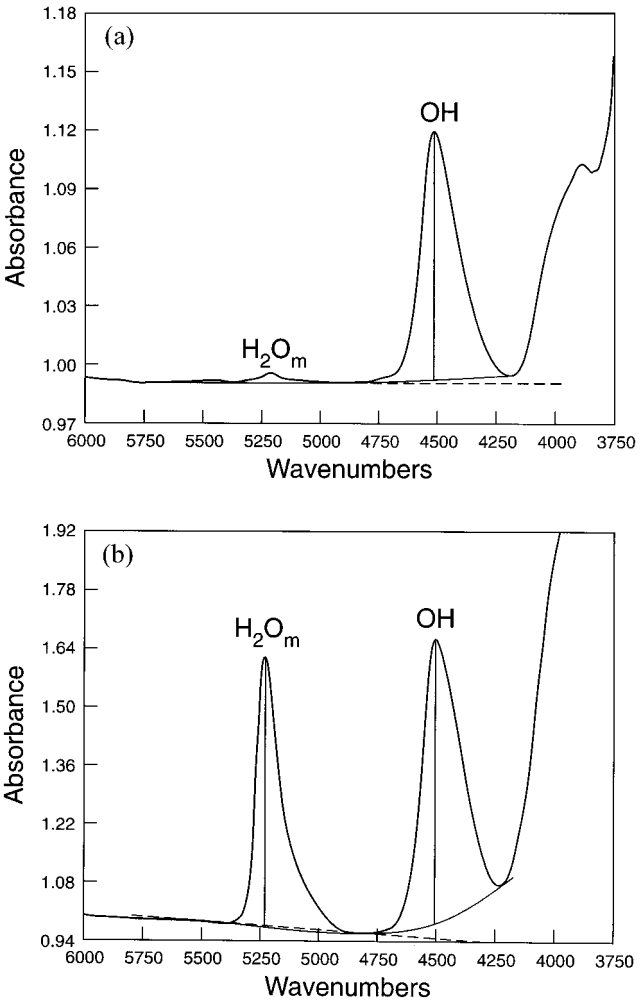

Figure 1. Infrared spectra of two hydrous rhyolitic glasses, showing the two peaks usually used in the determination of species and total H_2O concentrations. The sample in Figure 1a contains 0.172% H_2O_t. The sample in Figure 1b contains 2.64% H_2O_t. Baselines are fit with a flexicurve (shown as the curve) in this lab. Some labs use straight-line fits (also shown). Reprinted from *Zhang et al.* [1997a] with permission from Elsevier Science.

where O is an anhydrous oxygen. The equilibrium constant of the above reaction is

$$K_2 = \frac{[OH]^2}{[H_2O_m][O]}. \tag{2}$$

Similar to K_1, K_2 is not an equilibrium constant in the strict sense but is used as a proxy. Note that (R2) implies that OH is the dominant species at low H_2O_t and that the importance of H_2O_m gradually increases with increasing H_2O_t (Figure 2). This can be clearly shown from infrared spectra: The 5230 cm^{-1} band is often not detectable when H_2O_t is less than 0.2% and becomes more prominent with increasing H_2O_t (Figure 1). The exact H_2O_t concentration at which H_2O_m becomes the dominant species depends on K_2 (Figure 2). The species equilibrium has been investigated experimentally both by the in situ method and by the study of quenched

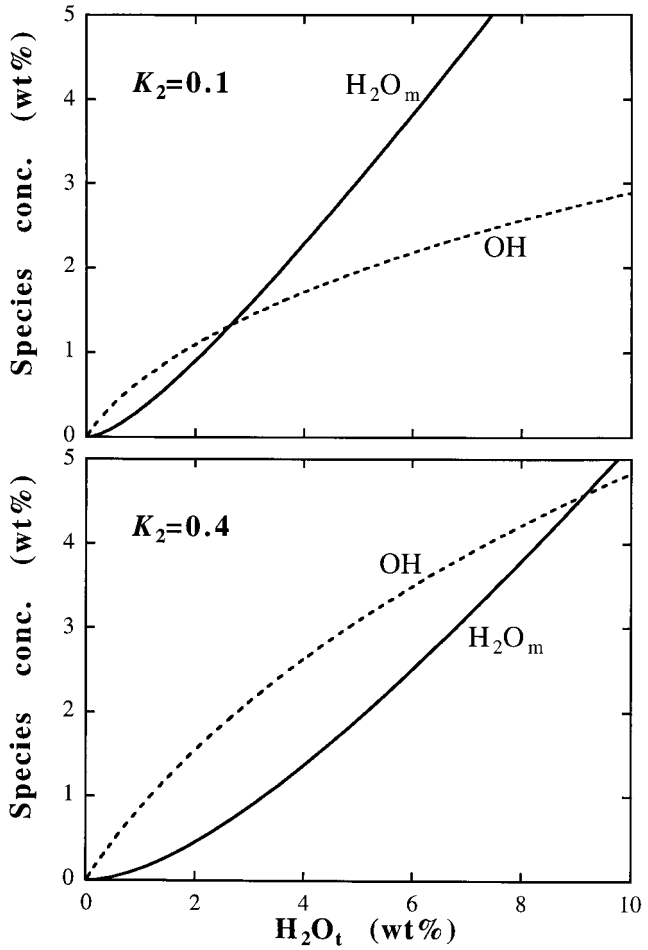

Figure 2. The dependence of H_2O_m and OH species concentrations on H_2O_t for two K_2 values. $K_2 = 0.1$ corresponds to 470°C, and $K_2 = 0.4°$ corresponds to 840°C. At low H_2O_t, OH is the dominant species. As H_2O_t increases, H_2O_m becomes increasingly more important and eventually dominant.

glasses. The equilibrium constant K_2 increases with temperature [*Ihinger*, 1991; *Zhang et al*., 1991a, 1995, 1997a; *Nowak and Behrens*, 1995; *Shen and Keppler*, 1995].

Understanding the speciation reaction is critical to the understanding of many phenomena about dissolved H_2O in silicate melts and glasses. Speciation plays an important role in the solubility of H_2O_t [e.g., *Blank et al*., 1993; *McMillan*, 1994]. At low H_2O pressures (P_{H_2O}), solubility of H_2O_t is low, and hence OH is the dominant species. Therefore H_2O_t solubility is roughly proportional to the square root of P_{H_2O}. At high P_{H_2O} the solubility of H_2O_t is high, and hence H_2O_m becomes significant. Therefore the H_2O_t solubility increases more rapidly than the square root of P_{H_2O}. The H_2O_t diffusivity in silicate melts and glasses is also affected by the species reaction. The two species, H_2O_m, which is neutral, and OH, which is charged or strongly bonded to other cations, are expected to have different diffusivities. Because H_2O_m/H_2O_t increases with H_2O_t, the H_2O_t diffusivity varies with H_2O_t. Furthermore, the speciation of H_2O also affects the fractionation of H isotopes between silicate melts and H_2O vapor [*Newman et al*., 1988; *Dobson et al*., 1989; *Ihinger*, 1991]. The data are consistent with a small D/H fractionation between dissolved H_2O_m in rhyolitic melt and H_2O in vapor and a large D/H fractionation between dissolved OH and H_2O in vapor. The speciation of H_2O also affects the thermodynamics of hydrous silicate liquids. In principle, speciation is also expected to affect viscosity and density.

The kinetics of the interconversion reaction between the species can be used as a geospeedometer [*Zhang et al*., 1995, 1997b]. Because a natural or experimental hydrous glass underwent continuous cooling (or even a more complex thermal history), and because the reaction rate constant for (R2) decreases with decreasing temperature, the final H_2O_m and OH concentrations for a given reaction in the glass at room temperature reflect the continuous reaction during the cooling history and were not established when the reaction reached equilibrium at a specific temperature. Hence the symbol Q (quotient) is sometimes used to refer to the final speciation, where $Q = [OH]^2/\{[H_2O_m][O]\}$ (the difference between Q and K_2 is that K_2 is the expression at equilibrium). A hypothetical equilibrium temperature can nonetheless be calculated from Q, which is referred to as the apparent equilibrium temperature T_{ae} [*Zhang*, 1994]. For example, if a hydrous magma is cooled continuously from 850°C to a glass at room temperature, the H_2O_m and OH species concentrations may record a T_{ae} of 500°C. For a fixed H_2O_t, slower cooling leads to smaller Q and lower T_{ae}. Such relations can be used to infer cooling rates and the cooling environment: High cooling rates often indicate quench in water or air, and low cooling rates indicate cooling in the volcanic conduit, in a lava flow, or in a buried layer of pyroclastic deposits.

1.4. Outline of This Paper

In the following sections I review the large amount of information on recent progress on H_2O in rhyolitic and quasi-rhyolitic melt and glass (Table 1). I concentrate on H_2O in rhyolitic and quasi-rhyolitic glasses and melts because this system is best studied in many aspects. In section 2 I review the infrared measurement of dissolved H_2O and species concentrations in rhyolitic glasses at room temperatures. In section 3 I review the equilibrium speciation and the in situ versus quenched speciation controversy and how the controversy can be reconciled. In section 4 I review the H_2O solubility data and models and present a new solubility model applicable to 0–8000 bars and 500°–1350°C. In section 5 I review H_2O diffusion, with a critical assessment of low versus high H_2O and low versus high T diffusion data. A simple expression for calculation of diffusivity of the H_2O component is also presented. The review will clarify some confusion in literature and point to new directions for future research.

2. MEASUREMENT OF DISSOLVED H_2O IN RHYOLITIC GLASSES AT ROOM TEMPERATURE

All the advances in our understanding of the role of H_2O in silicate liquids and glasses require accurate measurement of H_2O_t and/or species concentrations of H_2O_m and OH. Analytical methods for H_2O_t and species concentrations have been summarized by *Ihinger et al.* [1994]. There are two types of measurement techniques. In one type of technique, including manometry [e.g., *Newman et al.*, 1986] and Karl-Fischer titration [e.g., *De Jong et al.*, 1987; *Behrens*, 1995], dissolved H_2O is extracted from the solid material and then measured by either mass spectrometry or titration. The second type is nondestructive microbeam techniques, including vibrational spectroscopy in the infrared (IR) and near-infrared (NIR) regions, ion microprobe (SIMS), nuclear magnetic resonance spectroscopy (NMR), nuclear reaction analysis (NRA), and Raman scattering spectroscopy [*Mysen and Virgo*, 1986a, b; *McMillan et al.*, 1993; *Holtz et al.*, 1996]. In these techniques the dissolved H_2O component is not extracted (hence the sample is not destroyed) but is measured at spots (small areas) in the sample.

The different techniques are complementary, and each is useful in some aspects. The bulk extraction methods determine the absolute amount of H_2O_t and are often used to calibrate other (spectroscopic) techniques. However, the bulk extraction methods are time-consuming, destructive to the sample, unable to measure species concentrations, and unable to measure H_2O_t precisely below 0.2%. The NRA technique does not require calibration and is not destructive and is therefore very useful in calibrating other techniques. However, its precision is not very high ($\geq$5% relative [*Endisch et al.*, 1994]), and it cannot provide species information. Other microbeam techniques require calibration. The SIMS technique can analyze small spots and D/H ratios. In depth profiling, the SIMS technique has extremely high spatial resolution ($\leq$0.01 μm). However, it cannot determine species concentrations and is not as sensitive as the IR technique at low H_2O_t [*Ihinger et al.*, 1994]. The NMR technique has been used mostly to understand solubility mechanisms [*Farnan et al.*, 1987; *Kohn et al.*, 1989], but it has not been explored as a quantitative analytical tool. Even though Raman spectroscopy has the potential of determining the H_2O_m and OH species concentrations, it has not been calibrated, and its calibration is more difficult than that for the IR technique because of problems in determining cross sections.

Infrared (IR, including near-infrared, NIR) spectroscopy provides a rapid, nondestructive microbeam technique for quantitative analysis of H_2O_t and species concentrations with high precision and sensitivity. The more recent IR studies all use Fourier transform infrared spectroscopy (FTIR). At present, IR spectroscopy is the only method that is capable of precisely determining H_2O_t at low concentrations and determining the H_2O_m and OH species concentrations. In quantitative H_2O_m and OH determinations the two near-infrared bands at 4520 and 5230 cm^{-1} are most often used because the band intensities for typical geological samples are neither too large nor too small. For example, although the 3550 cm^{-1} band characterizes total H_2O_t and is often used to investigate H_2O at low H_2O_t (e.g., in minerals), the band intensity is usually too strong for quantitative investigation of H_2O in hydrous rhyolitic glasses with 0.1–7% H_2O_t. The absorbance would be too high (that is, too few photons at ~3550 cm^{-1} would reach the detector) unless H_2O_t is low or the sample thickness is made very thin (e.g., for a rhyolitic glass containing 5% H_2O_t, for the absorbance of the 3550 cm^{-1} band to be less than 2, the thickness must be <40 μm). Thin samples are easy to break, have larger thickness measurement errors, and are more prone to interference fringes. On the other hand, the 7100 cm^{-1} band is typically too weak except for very thick samples or samples with very high H_2O_t. The discussion below concerns calibration for measurement at room temperature. In situ measurement at high temperature will be discussed in the next section since no calibration has been published yet.

The IR measurements provide only vibrational band intensities in the IR region. Converting IR band intensities into species concentrations is based on Beer's law:

$$C = \frac{wA}{\varepsilon d \rho}, \tag{3}$$

where w is the molar mass of the component or species; A ($\equiv \log (I_0/I)$, with I_0 being the radiation transmitted without the species being measured and I being the radiation transmitted with the species present) is the absorbance; ε is the molar absorptivity; d is the thickness of the sample; and ρ is the density. Absorbance can be either in terms of the height of a peak or in terms of the total area under a peak. The molar absorptivity must be obtained through calibration because of the absence of a good theoretical understanding of the band intensities in glasses.

Because there are two H_2O species, the H_2O_t concentration can be expressed as [*Stolper*, 1982a; *Newman et al.*, 1986]

$$C = C_1 + C_2 = \frac{18.015\bar{A}_{523}}{\rho\varepsilon_{523}} + \frac{18.015\bar{A}_{452}}{\rho\varepsilon_{452}}, \tag{4}$$

where C, C_1, and C_2 are mass fractions of H_2O_t, H_2O_m, and OH, respectively, expressed as H_2O; $\bar{A} = A/d$; $\bar{A}_{523}$ and $\bar{A}_{452}$ are absorbances of the 5230 and 4520 cm^{-1} bands per millimeter sample thickness; ρ is the density and depends on H_2O_t (about 2340 g/L for a typical dry rhyolitic glass); and ε_{523} and ε_{452} are the molar absorptivities for the 5230 and 4520 cm^{-1} bands in L mol^{-1} mm^{-1} and depend on, among others, the anhydrous composition and how the baseline is fit (Figure 1) [*Behrens et al.*, 1998]. With the estimation of peak height or

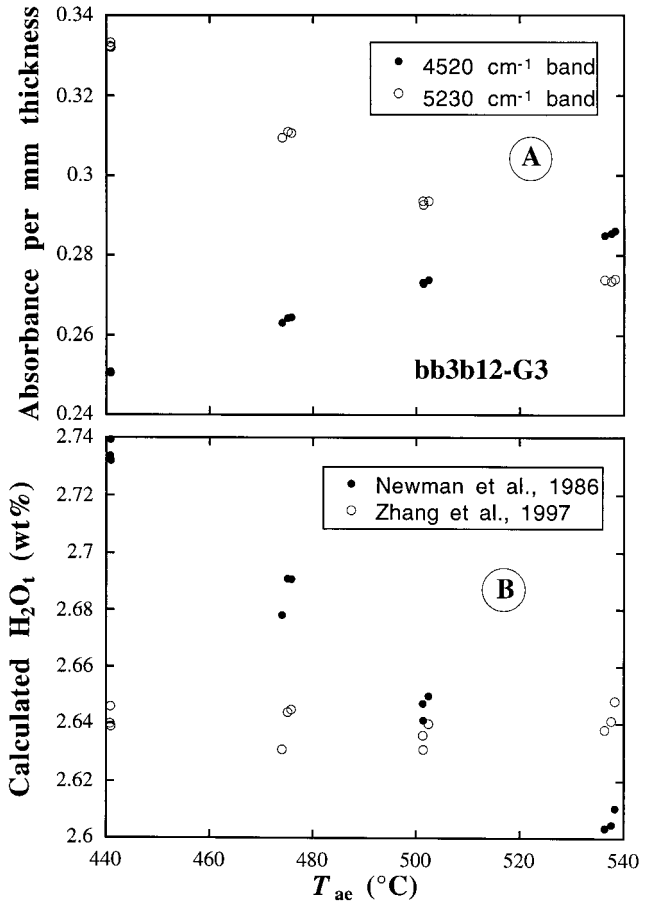

Figure 3. (a) The intensity variations of the 4520 and 5230 cm^{-1} bands upon heating. The horizontal axis is the apparent equilibrium temperature. The rhyolitic glass was heated to variable temperatures and quenched to room temperature for infrared measurement. (b) Calculated H_2O_t using two calibrations. The calibration of *Newman et al.* [1986] does not return a constant H_2O_t, whereas that of *Zhang et al.* [1997a] returns roughly constant H_2O_t, satisfying a necessary condition for an accurate calibration. Figure 3b is from *Zhang et al.* [1997a]. Reprinted with permission from Elsevier Science.

peak area ($\bar{A}_{523}$ and $\bar{A}_{452}$) from infrared spectra the determination of ε_{523} and ε_{452} (i.e., calibration) is carried out by determining C using an independent absolute method. The calibration is complicated because all absolute methods only determine H_2O_t, not H_2O_m and OH. Other bands (including the 1630, 3550, and 7100 cm^{-1} bands) can be calibrated similarly [*Newman et al.*, 1986].

Fitting the baseline for the infrared spectra (Figure 1) is not trivial. Three bands (the broad band at 3550 cm^{-1} and the 3900 and 4520 cm^{-1} bands) are convoluted at 4200 cm^{-1}, elevating the base on the right-hand side of the 4520 cm^{-1} band (Figure 1). The elevation at the 4200 cm^{-1} region is more pronounced as H_2O_t and/or measurement temperature increase. Owing to the elevation, there is still no objective way to obtain the true baseline. Two types of baselines (flexicurve and linear baselines) have been used in the literature (Figure 1). A third type of baseline is to use one tangential straight line for each peak and hence two straight lines (instead of a single straight line as shown in Figure 1) for two peaks. None of the baseline fits is entirely satisfactory in determining the true baseline and the true peak height (or peak area) of the 4520 cm^{-1} band. The difficulty in determining the true peak height may contribute to some of the variability of the molar absorptivities discussed below.

2.1. Calibrations by Assuming Constant Molar Absorptivities, and Problems

Stolper [1982a] calibrated the IR technique for natural and synthetic aluminosilicate glasses but noted the potential error in the "known" H_2O_t concentration values for his standard samples. *Newman et al.* [1986] recalibrated the IR technique by linear regression using a suite of rhyolitic glasses with $\leq$2.6% H_2O_t that were analyzed by manometry and IR, resulting in the widely used molar absorptivities $\varepsilon_{523} = 0.161$ and $\varepsilon_{452} = 0.173$ L mol^{-1} mm^{-1}. *Ihinger et al.* [1994] reported a revised set of molar absorptivities ($\varepsilon_{523} = 0.186$ and $\varepsilon_{452} = 0.150$ L mol^{-1} mm^{-1}) using additional manometry data at high H_2O_t to improve the accuracy at high H_2O_t. In all of these calibrations each molar absorptivity value for a given anhydrous composition was assumed to be constant, independent of H_2O_t and band intensities.

Possible problems with the calibrations of *Newman et al.* [1986] and *Ihinger et al.* [1994] were indicated by heating experiments. Because the equilibrium constant K_2 depends on temperature, the H_2O_m and OH concentrations (and hence the band intensities) for a given H_2O_t vary with the equilibrium temperature [e.g., *Zhang et al.*, 1991a, 1997a] (Figure 3) and hence thermal history. (When some heating steps did not reach equilibrium, the apparent equilibrium temperature could be used as a proxy for the equilibrium temperature.) One basic requirement for an accurate calibration is that calculated H_2O_t using the calibration should be constant for a piece of glass before and after heating if no H_2O is lost or gained. *Skirius et al.* [1990], *Zhang et al.* [1991a], and *Qin* [1994] noted that by using the calibration of *Newman et al.* [1986], the same samples may have either greater or smaller calculated H_2O_t after heating than before heating. These problems can be attributed to the inaccuracy of the calibration. Using data from kinetic experiments, *Zhang et al.* [1995] examined the molar absorptivity ratio ($\varepsilon_{523}/\varepsilon_{452}$) by rewriting (4) as

$$\bar{A}_{523} = \frac{\rho C}{18.015}\varepsilon_{523} - \frac{\varepsilon_{523}}{\varepsilon_{452}}\bar{A}_{452}. \quad (5)$$

Equation (5) suggests that by plotting $\bar{A}_{523}$ versus $\bar{A}_{452}$ for a single sample with fixed C (and hence ρ) but heated to different T, the molar absorptivity ratio can be obtained from the slope. *Zhang et al.* [1995] heated the same piece of rhyolitic glass to different T_{ae} so that $\bar{A}_{523}$

and $\bar{A}_{452}$ vary at constant ρC (layers affected by significant diffusive loss of H_2O_t were polished away before IR analyses). They found indeed that good straight lines were obtained in $\bar{A}_{523}$ versus $\bar{A}_{452}$ for a given sample with different thermal history and that $\varepsilon_{523}/\varepsilon_{452} \approx 1.6 \pm 0.3$, different from the ratio of 0.93 (= 0.161/0.173) of the calibration of *Newman et al*. [1986]. Hence the relative error in the calibration of *Newman et al*. [1986] for species concentrations is large.

2.2. Calibrations by Accounting for Variations of Molar Absorptivities

Zhang et al. [1997a] carried out a new calibration of the molar absorptivities by combining infrared/manometry measurements and a new FTIR study of hydrous rhyolitic glasses heated at different temperatures. Their heating experiments for constant H_2O_t show that (1) $\bar{A}_{523}$ versus $\bar{A}_{452}$ for the same glass wafer with the same H_2O_t but heated to different temperature is roughly a straight line, the slope of which gives the $\varepsilon_{523}/\varepsilon_{452}$ ratio for the sample; (2) the ratio $\varepsilon_{523}/\varepsilon_{452}$ varies with H_2O_t; and (3) the calculated H_2O_t using the calibration of *Newman et al*. [1986] for a glass with the same H_2O_t is not constant but depends on T_{ae} (Figure 3b). Therefore the earlier assumption of constant molar absorptivities is inaccurate. The accurate calibration must incorporate the variation of ε_{523} and/or ε_{452} with H_2O_t.

The variation of ε_{523} and/or ε_{452} could be explained in several ways. (1) Since ε_{523} and ε_{452} are expected to be constant only when H_2O_m and OH concentrations are dilute, the interaction among the H-bearing clusters at high concentrations may cause the variation. (2) There may be several subspecies of OH (or H_2O_m), such as Si-OH and AlOH or Q_3-OH and Q_2-$(OH)_2$ [*Farnan et al*., 1987; *Zotov and Keppler*, 1998], whose concentrations depend on H_2O_t and T_{ae}. The subspecies may have different molar absorptivities. The variation of their concentration ratios can lead to variable ε_{523} and ε_{452}. (3) The inaccuracy in determining the true peak height may contribute to part of the variation of ε_{452}. Whatever the reasons, the variation of ε_{523} and/or ε_{452} needs to be accounted for empirically. Because the functional dependence of ε_{523} and ε_{452} on species concentrations is not known from first principles, the choice of the functional form introduces arbitrariness into the calibration and may cause difficulty in extrapolation. For simplicity, *Zhang et al*. [1997a] defined

$$\delta_{523} = \frac{18.015}{\rho_0 \varepsilon_{523}} \qquad \delta_{452} = \frac{18.015}{\rho_0 \varepsilon_{452}}, \tag{6}$$

so that (4) can be linearized to the following form:

$$\frac{\rho}{\rho_0} C = \delta_{523} \bar{A}_{523} + \delta_{452} \bar{A}_{452}, \tag{7}$$

where ρ_0 is the density of the anhydrous rhyolitic glass and ρ is the density of the hydrous glass (a function of C) and $\rho/\rho_0 \approx 1 - C$. Then they assumed that each of δ_{523} and δ_{452} depends on both $\bar{A}_{523}$ and $\bar{A}_{452}$, where $\bar{A}_{523}$ and $\bar{A}_{452}$ are used as proxies for H_2O_m and OH. That is,

$$\delta_{523} = a_0 + a_1 \bar{A}_{523} + a_2 \bar{A}_{452}, \tag{8a}$$

$$\delta_{452} = b_0 + b_1 \bar{A}_{523} + b_2 \bar{A}_{452}, \tag{8b}$$

where a_0, a_1, a_2, b_0, b_1, and b_2 are fitting parameters. Preliminary fitting results show that a_1 and a_2 are close to zero. Hence they assumed that a_1 and a_2 are zero and refit the data to obtain the parameters (Table 2). Therefore the final expressions for calculating C (mass fraction of H_2O_t), C_1 (H_2O_m), and C_2 (mass fraction of H_2O present as OH) are

$$C(1 - C) = a_0 \bar{A}_{523} + (b_0 + b_1 \bar{A}_{523} + b_2 \bar{A}_{452}) \bar{A}_{452}, \tag{9a}$$

$$C_1 = a_0 \bar{A}_{523}/(1 - C), \tag{9b}$$

$$C_2 = (b_0 + b_1 \bar{A}_{523} + b_2 \bar{A}_{452}) \bar{A}_{452}/(1 - C). \tag{9c}$$

From an IR spectrum the right-hand side of (9a) can be calculated, and hence C can be solved from the quadratic equation. C_1 and C_2 can then be obtained from (9b) and (9c).

TABLE 2. Parameters for Calculation of H_2O_m and OH Concentrations in Rhyolitic Glass From 5230 and 4520 cm^{-1} Peak Heights

Parameter	*Value*
a_0, mm	0.04217 ± 0.0013
a_1, mm	0
a_2, mm	0
b_0, mm	0.04024 ± 0.0023
b_1, mm^2	−0.02011 ± 0.0051
b_2, mm^2	0.0522 ± 0.0051

Uncertainties are given at the 2σ level. The baseline is fit by a flexicurve.

2.3. Discussion

Comparison of the calibration of *Zhang et al*. [1997a] with that of *Newman et al*. [1986] shows that the calibration of *Newman et al*. [1986] is still good in retrieving H_2O_t within 5% relative precision, but not species concentrations. As shown in Figure 3, the calibration of *Zhang et al*. [1997a] has a high internal reproducibility in calculating H_2O_t for a sample heated to different temperatures (Figure 3) with a precision of about 0.7% relative, about a factor of 6 better (smaller) than that of *Newman et al*. [1986]. Owing to the input data range and the arbitrary choice of the functional dependence of molar absorptivities on band intensities, *Zhang et al*. [1997a] concluded that their calibration is most accurate for H_2O_t and species concentrations at ≤2.7% H_2O_t. One important contribution of this new calibration is to reveal that K_2 is independent of H_2O_t, at least up to 2.4% H_2O_t. This is contrary to the H_2O_t dependence of K_2 (modeled using a regular solution model [*Zhang et*

al., 1991a]) if the calibration of *Newman et al*. [1986] is used.

The work of *Zhang et al*. [1997a] is not the last word on the calibration of the IR measurement of H_2O in rhyolitic glasses. In terms of species concentrations their calibration may not be very accurate at $H_2O_t > 2.7\%$. Despite improvement in reproducibility, the accuracy in H_2O_t of their calibration is not significantly better than that of *Newman et al*. [1986], owing to uncertainties in manometry data. Recent work (Y. Zhang and H. Behrens, H_2O diffusion in silicate glasses and melts, submitted to *Chemical Geology*, 1999; hereinafter referred to as submitted manuscript, 1999) indicates that at $H_2O_t > 5.5\%$, the accuracy of the calibration of *Zhang et al*. [1997a] deteriorates rapidly, implying that the complicated formulation in (9) cannot be extrapolated. For example, calculated H_2O_t for a sample that contains 7.6% H_2O_t (by Karl-Fischer titration) is only 6.6% using *Zhang et al*. [1997a], 7.5% using *Newman et al*. [1986], and 6.9% using *Ihinger et al*. [1994]. Note that the calibration of *Newman et al*. [1986], although using samples containing only $\leq 2.3\%$ H_2O_t, agrees best with the Karl-Fischer-titration result at very high H_2O_t. Since *Ihinger et al*. [1994] used higher H_2O_t samples for calibration and assumed constant ε_{523} and ε_{452}, the discrepancy between the calibration of *Ihinger et al*. [1994] and Karl-Fischer titration may mean a discrepancy between the manometry method and Karl-Fischer titration for obtaining bulk H_2O_t.

At low H_2O_t ($<0.2\%$) the 5230 and 4520 cm^{-1} band intensities are weak. For example, for a sample containing 0.1% H_2O_t and with a thickness of 1 mm, the absorbance of the 4520 cm^{-1} band is ~0.024 absorbance unit and that of the 5230 cm^{-1} band is typically too small to resolve. Hence it is best to use the 3550 cm^{-1} band for determination of low H_2O_t. *Newman et al*. [1986], *Dobson et al*. [1989], and *Ihinger et al*. [1994] reported calibration of this band. However, the discrepancy is still large owing to the uncertainty in measuring H_2O_t by manometry at such low H_2O_t. For example, *Bagdassarov et al*. [1996] applied two different calibrations to obtain H_2O_t with a range of 0.12–0.16%.

In conclusion, much improvement in the calibration is still necessary for both high and low H_2O_t. It is also necessary to carry out an interlaboratory comparison of manometry and Karl-Fischer titration measurements. Some workers may think that we have reached a point of diminished returns. However, in my opinion, improving the calibration remains one of the high priorities in future work on water in silicate melts and glasses, because reliable calibration is a prerequisite for studies on H_2O speciation (such as how K_2 depends on H_2O_t), solubility, and diffusion.

2.4. Calibrations of the IR Technique for H_2O in Other Glasses

The infrared measurement of H_2O_t and species concentrations in other silicate glasses has also been calibrated [*Dixon et al*., 1988, 1995; *Silver and Stolper*, 1989; *Silver et al*., 1990; *Pandya et al*., 1992; *Danyushevsky et al*., 1993; *Behrens*, 1995; *Behrens et al*., 1996; *Nowak and Behrens*, 1997]. Published linear molar absorptivities and densities required for the calculation of species and H_2O_t concentrations using (4) (or a similar equation for other IR bands) for other glasses are listed in Table 3. All these other calibrations assumed H_2O_t-independent molar absorptivities, and none of them has been subjected to the same kind of scrutiny as the calibration for rhyolitic glasses. Therefore they may have potential problems similar to those of the calibration of *Newman et al*. [1986], although this has not been demonstrated yet. Some calibrations are based on a curve fit to the baseline using a flexicurve (solid curves in Figure 1), and some are based on a straight-line fit to the baseline (dashed lines in Figure 1). For self-consistency the baseline fitting procedure must follow that used in the calibration for calculation of H_2O_t, H_2O_m, and OH concentrations. Note that density determination is for glasses prepared and quenched at high pressures, and hence the densities are somewhat greater than those at 1-bar pressures.

3. EQUILIBRIUM SPECIATION OF H_2O IN SILICATE GLASSES AND MELTS

Understanding the equilibrium speciation of H_2O in silicate glasses and melts is critical to modeling the thermodynamic properties of silicate melts, understanding solubility, diffusion, and H isotopic fractionation, inferring apparent equilibrium temperature of a glass, and setting the stage for kinetic studies. There are two experimental approaches for studying the equilibrium speciation of H_2O as a function of temperature (and pressure) and H_2O_t content. One method is to hold the silicate glass at high temperature to reach equilibrium and then rapidly quench it to room temperature [*Silver and Stolper*, 1989; *Silver et al*., 1990; *Stolper*, 1989; *Ihinger*, 1991; *Zhang et al*., 1991a, 1995, 1997a]. The species concentrations in the quenched glass are then measured at room temperature by IR. This approach will be referred to as the quench technique hereinafter. The other method of characterizing high-temperature speciation is the in situ method, in which the species concentrations are measured in situ as the sample is held at high temperature and pressure [*Nowak and Behrens*, 1995; *Shen and Keppler*, 1995]. The disagreements between earlier and more recent speciation data using the quench technique [*Silver and Stolper*, 1989; *Silver et al*., 1990; *Stolper*, 1989; *Ihinger*, 1991; *Zhang et al*., 1991a, 1997a, b; *Ihinger et al*., 1999], the changes in calibration, and the disagreement between data using the quench and the in situ techniques [e.g., *Zhang et al*., 1991a, 1995, 1997a, b; *Nowak and Behrens*, 1995; *Shen and Keppler*, 1995] have caused much confusion in understanding the true speciation in silicate glasses and melts. Different

TABLE 3. Linear Molar Extinction Coefficients for H_2O Species in Glasses

	1.91 μm, 5230 cm^{-1}, H_2O_m	*2.21 μm, 4520 cm^{-1}, OH*	*2.82 μm, 3550 cm^{-1}, H_2O_t*	*6.13 μm, 1630 cm^{-1}, H_2O_m*	*Calibration H_2O_t Range, wt %*	*Density,*[a] *g L^{-1}*	*Reference*
Calibrations Using Flexicurve Fits to the Baseline (Straight Line for the 2.82-μm Band)							
Rhyolite	see text	see text			0.1–5.3%	not needed	1
Rhyolite	0.161	0.173		5.5 ± 0.2		2350/(1 + 0.31*X*)	2
Rhyolite			8.8 ± 0.2		0–0.4%	2350/(1 + 0.31*X*)	3
Rhyolite			8.0 ± 0.4		0–0.4%	2350/(1 + 0.31*X*)	4
Basalt	0.062	0.067	6.3	2.5			5, 6
Basalt			6.1	1.6			7
Basalt			6.06				8
Basanite	0.056	0.058					4
$NaAlSi_3O_8$(Ab)	0.167	0.113	7.0 ± 0.2	4.9 ± 0.2		measured	9
$NaAlSi_2O_6$	0.113	0.112				see reference 10	10
$KAlSi_3O_8$(Or)	0.187	0.143				see reference 10	10
$CaAl_2Si_2O_8$	0.150	0.120				see reference 10	10
Calibrations Using Straight-Line Fits to the Baseline							
AOQ	0.179	0.156			1.0–8.7%	2363 (1–0.61*C*)	11
$NaAlSi_3O_8$(Ab)	0.149	0.128			1.2–10.2%	2384 (1–0.58*C*)	12
Ab90Or10	0.147	0.126			2.4–7.3%	2389 (1–0.59*C*)	13
Ab70Or30	0.143	0.148			1.7–6.9%	2386 (1–0.62*C*)	13
Ab50Or50	0.149	0.157			1.6–7.1%	2390 (1–0.5*C*)	13
Ab30Or70	0.151	0.158			2.1–5.7%	2373 (1–0.5*C*)	13
Ab10Or90	0.156[b]	0.159[b]			···	···	13
$KAlSi_3O_8$(Or)	0.165	0.158			1.6–5.3%	2395 (1–0.67*C*)	13
$LiAlSi_3O_8$	0.112	0.132			2.2–13.3%	2382 (1–0.8*C*)	13
$Li_{.5}K_{.5}AlSi_3O_8$	0.136	0.124			1.0–7.2%	2379 (1–0.45*C*)	13
$Li_{.5}Na_{.5}AlSi_3O_8$	0.133	0.119			0.9–7.4%	2373 (1–0.48*C*)	13
Calibrations Using Programs to Curve Fit the Baseline and Peaks (Straight Line for the 2.82-μm Band)							
High-Al basalt	0.084	0.085	6.4 ± 0.1		1.1–3.7%	measured	14
Dacite	0.094	0.16	6.8 ± 0.1		1.4–3.0%	measured	14

Unit of molar absorptivities is L mol^{-1} mm^{-1}. References are 1, *Zhang et al*. [1997a]; 2, *Newman et al*. [1986]; 3, *Dobson et al*. [1989]; 4, *Ihinger et al*. [1994] (these values were listed without giving details); 5, *Dixon et al*. [1988]; 6, *Dixon et al*. [1995]; 7, *Pandya et al*. [1992]; 8, *Danyushevsky et al*. [1993]; 9, *Silver and Stolper* [1989]; 10, *Silver et al*. [1990]; 11, *Nowak and Behrens* [1997]; 12, *Behrens* [1995]; 13, *Behrens et al*. [1996]; and 14, *Yamashita et al*. [1997].

[a]In the density expression, *C* is mass fraction of H_2O_t, and *X* is mole fraction of H_2O_t on a single-oxygen basis.

[b]Obtained by interpolation.

experimental approaches and results are discussed below.

3.1. Experimental Data Obtained From the Quench Technique

The quench technique used in the earlier IR studies [*Silver and Stolper*, 1989; *Silver et al*., 1990] should be clearly distinguished from that used in more recent studies [*Ihinger*, 1991; *Zhang et al*., 1991a, 1995, 1997a, b; *Ihinger et al*., 1999]. Reaction (R2) is a homogeneous reaction and does not require mass transfer over micrometer distance. Hence the reaction can continue and can significantly alter the speciation even in the short timescale of quenching. If the species concentrations vary significantly during a quench, measured concentrations do not represent those at the experimental temperature, a problem typically referred to as the quench problem. *Silver and Stolper* [1989] and *Silver et al*. [1990] carried out extensive experimental work on the equilibrium of (R2). They held natural rhyolitic and other silicic samples at 800°–1400°C and quenched the samples to room temperature for infrared analyses. All workers in this field, including the authors of these studies [*Silver and Stolper*, 1989; *Silver et al*., 1990], now agree that these data suffered from a significant quench problem, as first pointed out by *Dingwell and Webb* [1990] on the basis of glass relaxation theory and later demonstrated by *Zhang et al*. [1995] using experimental data on the kinetics of the reaction. The quench problem arises because reaction rates at ≥700°C are extremely high and reaction continues during quench. Although most data of *Stolper* [1989] using the quench technique were at $T \leq 600$°C and were hence not affected by this quenching problem, Stolper used other quench data from ≥800°C in formulating an expression for K_2. The numeric models for the dependence of K_2 on H_2O_t and *T* [*Silver and Stolper*, 1989; *Stolper*, 1989; *Silver et al*., 1990] are invalid because of the use of the data with significant quench problems. These data and models are excluded from the following discussion.

Experimental data using the rapid quench technique discussed below are obtained at relatively low experi-

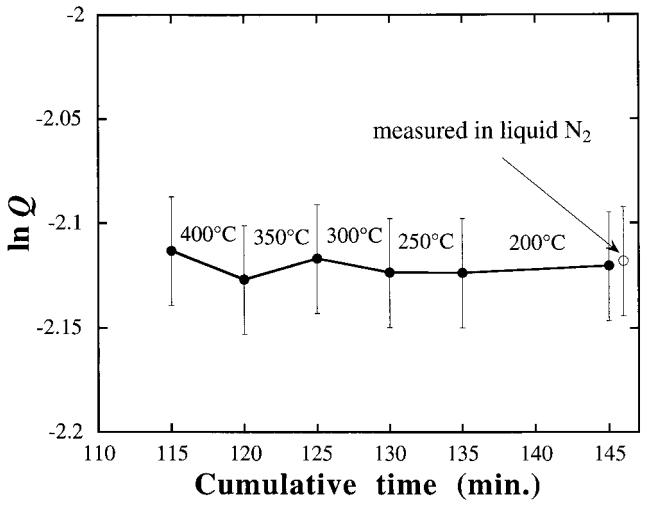

Figure 4. Examination of whether quenched species concentrations change when heated at sufficiently low temperatures. Data are from *Zhang et al*. [1995], but species concentrations are recalculated using the calibration of *Zhang et al*. [1997a].

mental temperatures, 400°–600°C [*Ihinger*, 1991; *Zhang et al*., 1991a, 1995, 1997a; *Ihinger et al*., 1999]. At these temperatures the reaction timescale is minutes to hours depending on H_2O_t and T [*Zhang et al*., 1995], much longer than the quench timescale (a few seconds) for rapid quench. Furthermore, *Zhang et al*. [1991a, 1995, 1997a, b], *Ihinger* [1991] and *Ihinger et al*. [1999] compared the reaction timescale and quench timescale case by case and excluded data that might have been affected by quench (such as $\geq$2.5% H_2O_t at 600°C). Therefore these data do not suffer from the above obvious quench effect. These authors also tested possible quench effects in several ways. One of the tests is to examine directly whether speciation may change when the experimental temperature is sufficiently low. *Zhang et al*. [1995] heated a hydrous glass to 400°, 350°, 300°, 250°, and 200°C for 5–10 min. The quenched speciation does not vary (Figure 4), implying that reaction rates at these temperatures are negligible. A second test is to see if the final speciation changes with quench rate if the initial temperature is sufficiently low. *Zhang et al*. [1997b] cooled a sample from 300°C slowly at 1°C min^{-1} and rapidly in liquid nitrogen and found no difference in the final speciation. They concluded that the quench effect is negligible in these quench data unless there is a portion of the reaction that is unquenchable (i.e., a portion of the reaction would continue to reach equilibrium at room temperature). The presence of such a portion of the reaction would not affect the inference of the apparent equilibrium temperature [*Zhang et al*., 1991a, 1995, 1997a] and cooling rate [*Zhang et al*., 1995, 1997b] but would affect the understanding of the true species concentrations at high T, the modeling of solubility data, and the values of molecular H_2O_m diffusivity.

Although the experimental IR data at 400°–600°C remain the same [*Zhang et al*., 1991a, 1995], the expression for K_2 from the speciation data using the quench technique has evolved with time [*Zhang et al*., 1991a, 1997a], owing to the improvement in calibration. Using the calibration of *Zhang et al*. [1997a], the equilibrium coefficient K_2 (see equation (2)) in a rhyolitic glass and melt at $H_2O_t \leq 2.4\%$ and 400°–600°C is independent of H_2O_t content and can be expressed as

$$K_2 = 6.53e^{-3100/T}. \quad (10)$$

The pressure dependence of K_2 is small at 550°C and $P \leq 10$ kbar [*Zhang*, 1993; *Ochs and Lange*, 1997]. At higher H_2O_t, up to 6% [*Ihinger et al*., 1999], the experimental data can be modeled either by an ideal mixing model if uncertainty in infrared calibration is allowed or by a regular solution model.

One disadvantage of the quench technique compared with the in situ technique is that only a small temperature range (400°–600°C) can be investigated, because the reaction rate is too slow at lower temperatures and too high (and hence the speciation is unquenchable) at higher temperatures. One advantage of the quench technique is that the IR technique is extensively calibrated only at room temperature (see previous section), and measurement at room temperature is simple and hence less prone to technical complications.

3.2. Experimental Data Obtained From the in Situ Technique

Nowak and Behrens [1995] and *Shen and Keppler* [1995] developed the in situ technique for determining equilibrium speciation under high T and high P. Compared with the simple quench technique, the in situ technique is more sophisticated and appealing. Since the sample is measured in situ at the high T and high P experimental conditions, an obvious advantage is that there is no quench effect and so the method provides actual band intensities at high temperatures and pressures (although one must still be careful to ensure that equilibrium is attained). Furthermore, it can be used to study speciation over a wide temperature range. The technique hence has great potential if molar absorptivities do not vary with measurement temperature and pressure. However, the technique also suffers from several disadvantages, including the following: (1) Technical difficulties for the in situ measurements mean that the precision is usually not as good as the room temperature measurements. (2) The possible variation of the molar absorptivities with temperature must be quantified. *Nowak and Behrens* [1995] and *Shen and Keppler* [1995] assumed that the molar absorptivities are independent of measurement T, but this is by no means proven. (3) Even if data from this method indicate actual speciation at high temperatures, if they are different from the quenched speciation, they are not directly applicable to estimation of the temperature or cooling rate recorded by the reaction in naturally or experimentally quenched glasses.

The in situ infrared spectra have been taken for two

hydrous glasses: a hydrous AOQ melt/glass (Table 1) containing 4.14% H_2O_t [*Nowak and Behrens*, 1995] and a hydrous potassic aluminosilicate melt/glass (composition 3 in Table 1) containing 8.1% H_2O_t [*Shen and Keppler*, 1995]. The AOQ composition used by *Nowak and Behrens* [1995] is similar to a rhyolitic composition and will be referred to as quasi-rhyolitic. Because *Shen and Keppler* [1995] used a glass with composition very different from that of rhyolite and did not report the original band intensities, their data are not included in the following discussion. However, owing to the similarity of the data between the two in situ studies, the conclusions based on the work of *Nowak and Behrens* [1995] are expected to be equally applicable to the work of *Shen and Keppler* [1995]. The available in situ data do not yet allow the examination of the dependence of K_2 on H_2O_t.

Nowak and Behrens [1995] showed that the intensities of the 5230 and 4520 cm^{-1} bands vary in the glass state at ≤400°C. The variations can be caused by either the true variation of speciation concentrations with temperature, which is unexpected, or the temperature dependence of molar absorptivities. The authors assumed that the molar absorptivities are constant and suggested that the variations imply that a portion of the speciation reaction is unquenchable. At higher temperatures the band intensities vary more rapidly with temperature. Again by assuming constant molar absorptivities, they calculated K_2 values as a function of T, shown in Figure 5. When compared with quenched speciation data, not only do the K_2 values differ, but the slopes in ln K_2 versus $1/T$ (i.e., the inferred enthalpy of reaction (2)) also differ significantly. *Nowak and Behrens* [1995] and *Shen and Keppler* [1995] concluded that the quench technique cannot be used to investigate equilibrium speciation for (R2). The validity of this claim is discussed below.

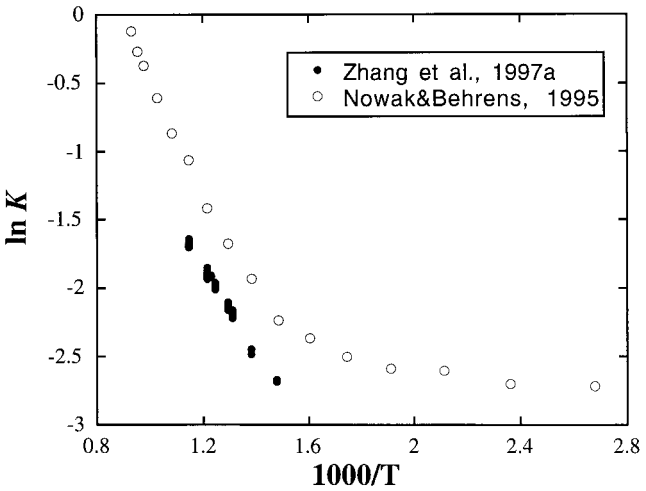

Figure 5. A comparison of equilibrium coefficient K_2 from two studies [*Zhang et al.*, 1997a; *Nowak and Behrens*, 1995]. The data are as reported by the authors without any reinterpretation.

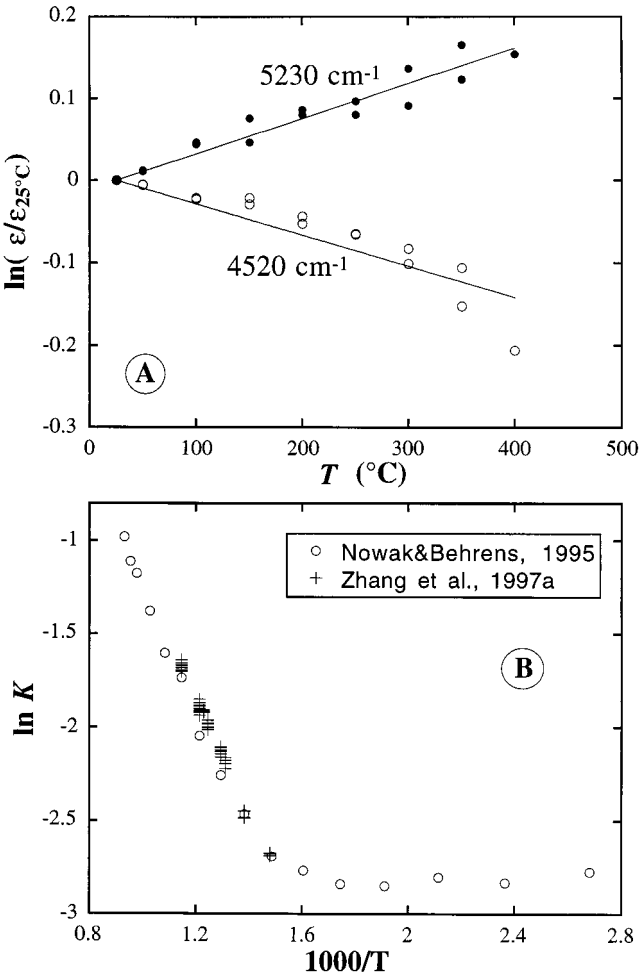

Figure 6. Reinterpretation of the in situ speciation data [*Nowak and Behrens*, 1995] in Figure 5 and comparison with the quench speciation data of *Zhang et al.* [1997a]. (a) Molar absorptivity divided by that at 25°C versus T for the 5230 and 4520 cm^{-1} bands. (b) Value of ln K_2 versus $1/T$, where species concentrations from *Nowak and Behrens* [1995] are recalculated using extinction coefficients in Figure 6a. See text for details. Reprinted from *Zhang* [1999] with permission from Elsevier Science.

3.3. Discussion

There is a large difference between the in situ data (assuming constant molar absorptivities) and the quenched data (Figure 5). I present the following reinterpretation of the in situ data [*Zhang*, 1999], which reconciles the difference between the two experimental techniques. Assuming that the band intensity variation with temperature at 0°–400°C [*Nowak and Behrens*, 1995] is caused by the temperature dependence of the molar absorptivities, this dependence can be obtained using original band intensity data (Figure 6a). A simple linear extrapolation of ln ($\varepsilon/\varepsilon_{25°C}$) versus T is used to extrapolate absorptivities at high T. Using these absorptivities, the "actual" species concentrations are calculated (although the accuracy may not be high). When the resulting K_2 values are compared with the data of *Zhang*

et al. [1997a], the agreement is very good (Figure 6b). More recent experimental data show that (1) IR molar absorptivities do vary with measurement temperature [*Behrens et al*., 1998; *Grzechnik and McMillan*, 1998; *Zhang and Behrens*, 1998a; A. C. Withers et al., Reconciliation of experimental results on H_2O speciation in rhyolitic glass using in situ and quenching techniques, submitted to *Earth and Planetary Science Letters*, 1999] and (2) Raman band shapes also change with temperature [*Holtz et al*., 1996] and hence support the above reinterpretation. How rapidly the molar absorptivities vary with temperature depends on whether the baseline is fit by a straight line or by a curve (Figure 1). There is no theoretical basis for the prediction of molar-absorptivity variation with temperature. Hence, although the in situ technique has many advantages and may represent the future of infrared study of H_2O in silicate melts and glasses, quantitative application of the technique must await the determination of the dependence of molar absorptivities on measurement temperature.

In conclusion, speciation data obtained from the quench technique do not suffer from a quench problem as long as the experimental temperature is not too high. On the other hand, quantification of in situ data requires calibration of the IR technique at the measurement temperatures. At present, (10) is the best representation of the dependence of K_2 with temperature at $H_2O_t \leq 2.4\%$ and $P \leq 5$ kbar.

4. H_2O SOLUBILITY IN RHYOLITIC MELT

A quantitative understanding of H_2O solubility (dissolved H_2O_t content in equilibrium with an H_2O pressure) in silicate melts is necessary for understanding the conditions under which H_2O exsolves in volcanic eruptions and the exsolution of a hydrothermal fluid that is important to the formation of ore deposits. Solubility of H_2O is expected to increase with P_{H_2O}, but not proportionally to P_{H_2O} because of the species reaction (R2). The dependence of H_2O solubility on temperature at a given pressure is more complicated because H_2O_m is expected to decrease with temperature (K_1 decreases with temperature) and OH is expected to increase with temperature (K_2 increases with temperature).

Early experimental work [e.g., *Goranson*, 1938; *Tuttle and Bowen*, 1958; *Shaw*, 1963; *Kadik et al*., 1972] demonstrated the high solubility of H_2O compared with other volatile components such as CO_2 and noble gases. Although H_2O solubility increases with pressure, it is not proportional to P_{H_2O} (or f_{H_2O}). The solubility coefficient (the concentration of H_2O_t in the melt divided by that of H_2O in the equilibrium vapor phase, or mole fraction of H_2O_t in the melt divided by f_{H_2O}) depends on f_{H_2O}. The nonconstancy of the solubility coefficient is largely caused by the formation of OH groups by the reaction of H_2O with the network oxygen. OH is the dominant species at low H_2O_t [*Burnham and Davis*, 1974] and becomes less dominant (but still significant) at high H_2O_t [*Stolper*, 1982b]. Our current understanding is that H_2O_t solubility is roughly proportional to $(P_{H_2O})^{1/2}$ at low P_{H_2O} ($\leq$2 kbar) because OH is the dominant species, but it increases more rapidly with further increase of P_{H_2O} because H_2O_m becomes an important species. *McMillan* [1994] reviewed H_2O solubility models. *Papale* [1997] and *Moore et al*. [1998] summarized H_2O solubility data and modeled the compositional dependence of H_2O solubility in a wide range of natural melt compositions. Other workers also investigated the compositional dependence of H_2O solubility in synthetic silicate melts [e.g., *Holtz et al*., 1992, 1995; *Behrens*, 1995]. The following discussion, however, concentrates on rhyolitic and quasi-rhyolitic melts.

4.1. Solubility Data

Various workers have reported experimental data on H_2O solubility in rhyolitic and quasi-rhyolitic melts [*Kadik et al*., 1972; *Khitarov and Kadik*, 1973; *Shaw*, 1974; *Dingwell et al*., 1984; *Silver et al*., 1990; *Ihinger*, 1991; *Holtz et al*., 1992, 1995; *Blank et al*., 1993; *Moore et al*., 1995, 1998]. In spite of these efforts, the data for H_2O solubility in rhyolitic melts as a function of temperature and pressure are still limited for the following reasons:

1. In the earlier studies the measurement of dissolved H_2O_t was not as accurate as in more recent work, especially at low H_2O_t. For example, *Jambon et al*. [1992] showed that the H_2O_t is 0.114% for a glass for which *Shaw* [1974] reported 0.38% H_2O_t. Hence there may be a discrepancy in the earlier and more recent data. There may also be other experimental problems in the earlier studies. Even in more recent studies, the slow-quench data of *Silver et al*. [1990] show more scatter than their rapid-quench data, and the solubility data of *Ihinger* [1991] also show considerable scatter (e.g., Figure 7a).

2. Few studies examined the temperature dependence of the H_2O solubility in silicate melts. The earlier experimental data were at 1200°C [*Kadik et al*., 1972; *Khitarov and Kadik*, 1973]. Most recent experimental data on rhyolitic melts were at 850°C. Only *Holtz et al*. [1992, 1995] examined the temperature dependence systematically for an AOQ (Qz28Ab38Or34) melt (composition 2 in Table 1). *Ihinger* [1991] reported two data points at 750°C in addition to data at 850°C for rhyolitic melts (composition 1 in Table 1).

3. The investigated pressure range of the H_2O solubility in silicate melts is still limited, mostly from 100 to 2000 bars. Most of the solubility data in rhyolitic and quasi-rhyolitic melts at pressures greater than 2 kbar were reported by *Holtz et al*. [1995] for the AOQ melt (Table 1). (Interestingly, the H_2O solubility in this melt was most extensively studied covering the widest range of T and P.) Besides their study, there are only five data points at higher pressures and two data points at lower pressures. Low-pressure solubility data are important, not only because they constrain solubility models and exsolution enthalpy, but also because H_2O exsolution at

low pressures is important for understanding explosive volcanic eruptions. There is hence a need for H_2O solubilities at both lower pressures (1–100 bars) and higher pressures (>2 kbar). At pressures greater than 5 kbar, because of bubble formation in melts containing very high H_2O_t during quench [*Holtz et al*., 1995], it may be necessary to use the in situ technique to determine H_2O solubility [*Shen and Keppler*, 1997].

Figure 7a compares reported experimental solubility data in rhyolitic melt at 850°C [*Shaw*, 1974; *Silver et al*., 1990; *Ihinger*, 1991; *Blank et al*., 1993]. H_2O_t from IR spectra are all recalculated using the new calibration [*Zhang et al*., 1997a]. Data from manometry or Karl-Fischer titration are directly used. The consistency between different laboratories is good. However, there is still considerable scatter, much greater than the analytical uncertainty. Such scatter leads to difficulties in using solubility data to test solubility models and to extract thermodynamic properties.

4.2. Modeling the Solubility Data

Burnham [1975], *Silver and Stolper* [1985], *Ihinger* [1991], *Blank et al*. [1993], *Holtz et al*. [1995], and *Moore et al*. [1998] modeled H_2O solubility in silicate melts. These models can be classified into three types: (1) assuming all dissolved H_2O dissociates to OH groups [*Burnham*, 1975, 1994]; (2) ignoring the role of speciation in H_2O solubility [*Moore et al*., 1995, 1998; *Papale*, 1997]; and (3) accounting for the role of two dissolved H_2O species [*Silver and Stolper*, 1985; *Ihinger*, 1991; *Blank et al*., 1993; *Holtz et al*., 1995].

The model of *Burnham* [1975] was developed before establishment of H_2O speciation in silicate melts. The model assumes that the activity of H_2O_t is proportional to the square of H_2O_t mole fraction (i.e., it implicitly assumes that all dissolved H_2O dissociates to OH groups) at $H_2O_t \leq 6.4\%$ and a complicated empirical function at greater H_2O_t. The equilibrium constant for the solubility coefficient is a polynomial function of T and ln P calibrated from measured solubility and partial molar volume of H_2O_t. The model works well at low pressures but less satisfactorily at high pressures. For example, at 1100°C and 5 kbar for the AOQ melt, using the adjustable parameter of 5.13 [*Burnham*, 1994] to account for 28% SiO_2 component in the melt, the calculated solubility using the Burnham model is 8.4%, lower than the experimental 10.8% of *Holtz et al*. [1995].

In two recent papers, *Moore et al*. [1995, 1998] obtained H_2O solubility data for a wide range of natural melt compositions. They fit the experimental solubility data using the following equation:

$$2 \ln X_{H_2O_t}^{melt} = \frac{2565}{T} - 14.21 + 1.171 \ln f_{H_2O} + \frac{P}{T}(2.736X_{Na_2O} - 1.997X_{Al_2O_3} - 0.9275X_{FeOt}),$$

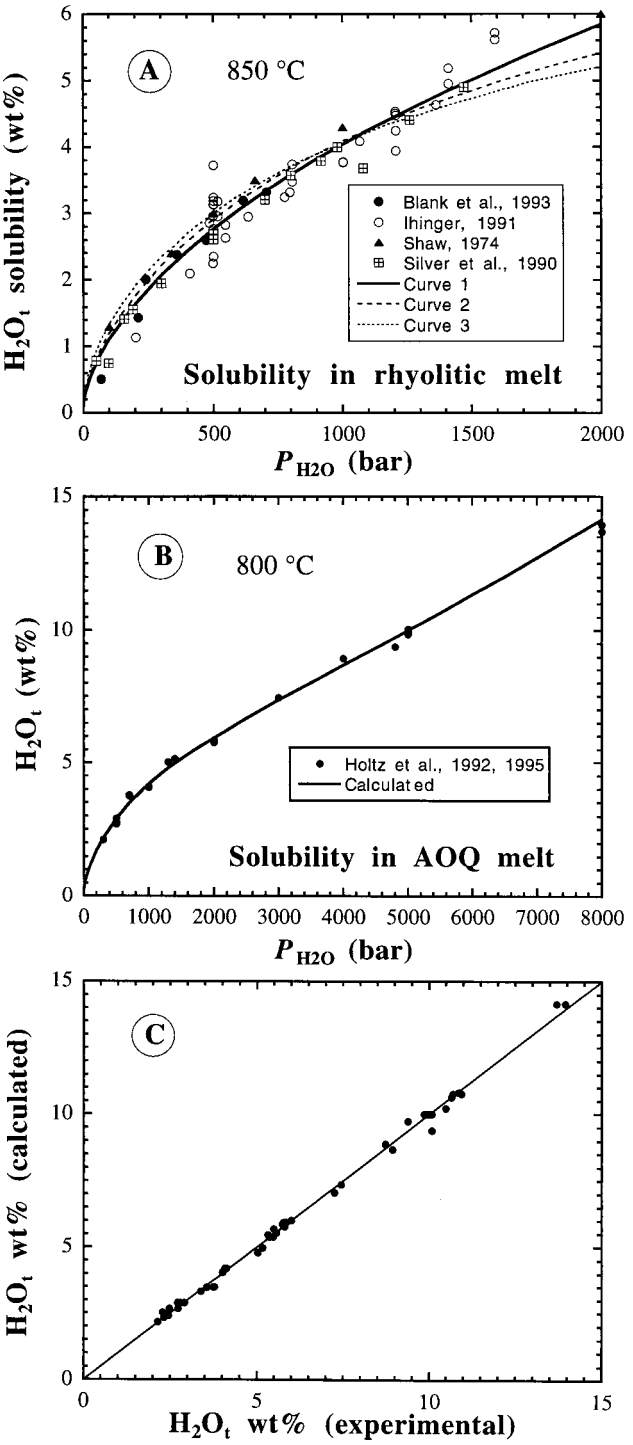

Figure 7. Comparison of experimental solubility data on rhyolitic and AOQ melts and solubility models. (a) Experimental solubility data on natural rhyolitic melt. The calculated curve 1 uses K_1 from equation (14) and K_2 from equation (10). Curves 2 and 3 are produced using K_1 from equation (17) with the H_2O molar volume of *Ochs and Lange* [1997] and K_2 of either the present work or *Nowak and Behrens* [1995]. (b) Comparison of experimental and calculated solubility for the quasi-rhyolitic AOQ (Qz28Ab38Or34) melt at 800°C using K_1 from equation (14) and K_2 from equation (10). (c) Comparison of all experimental solubility data for the AOQ melt with calculation using K_1 from equation (14) and K_2 from equation (10). The solid line is the 1:1 line.

where $X^{melt}_{H_2O_t}$, $X_{Al_2O_3}$, X_{FeO_t}, and X_{Na_2O} are the mole fractions on an oxide molar basis, P is in bars, and T is in kelvins. *Papale* [1997] constructed a regular solution model to account for the effect of anhydrous melt composition on H_2O solubility. The models of *Papale* [1997] and *Moore et al*. [1998] fill a gap for prediction of solubility over a wide range of compositions, but both ignored the role of speciation in H_2O solubility. The model of *Papale* [1997] lacks details for calculation, is difficult to use, and hence will not be discussed further. The model of *Moore et al*. [1998] can predict solubility data in the intermediate pressure range (100–3000 bars) very well. However, owing to its empirical nature (especially the 1.171 $\ln f_{H_2O}$ term, implying that the activity of H_2O_t is proportional to the 1.7th power of H_2O_t mole fraction), the formulation does not account for the effect of H_2O_m and OH species and has large relative errors at $P > 3$ kbar (as cautioned by the authors themselves).

The models of *Silver and Stolper* [1985], *Ihinger* [1991], *Blank et al*. [1993], and *Holtz et al*. [1995] account for the role of two species and hence have more potential for accurately predicting H_2O solubilities in a wide range of T and P. The solubility is the summation of two terms: dissolved H_2O_m, whose concentration is related to the H_2O fugacity through (R1), and OH groups, whose concentration is related to the H_2O_m concentration through (R2). Following these workers, I present an updated model for H_2O solubility in rhyolitic and quasi-rhyolitic melts using the new speciation model (equation (10)). From the model results, the thermodynamic consistency of solubility, speciation, and other available data is evaluated.

Because species concentrations depend on H_2O_t that depends on P_{H_2O}, the H_2O fluid pressure affects solubility in two ways: (1) pressure effect on equilibrium constants of (R1) and (R2), reflected in partial molar volumes, and (2) pressure effect on H_2O_t concentration that affects the relative species concentrations (Figure 2). Temperature affects the equilibrium constants of both (R1) and (R2) and hence the solubility. Total solubility of H_2O can be expressed as

$$[H_2O_t] = [H_2O_m] + 0.5[OH] = K_1 f + 0.5(K_1K_2f[O])^{1/2}, \quad (11)$$

where f is the fugacity of H_2O, K_1 depends on both T and P, and K_2 depends only on T at pressures below 10 kbar. In calculating f, the vapor phase in equilibrium with the melt at high T and P is assumed to be pure H_2O. Because the anhydrous components (Na_2O, K_2O, SiO_2, etc.) can dissolve in the vapor phase, especially at high T and high P, it is expected that the error of this assumption increases with both temperature and pressure, but the effect cannot be quantitatively estimated at this time. Knowing K_2 and $[H_2O_m]$ (equal to $K_1 f$), [OH] in (11) can be solved from (2) and $[H_2O_m] + [OH] + [O] = 1$, leading to

$$[H_2O_t] = K_1 f + \frac{K_1K_2f(1 - K_1f)}{K_1K_2f + [(K_1K_2f)^2 + 4K_1K_2f(1 - K_1f)]^{1/2}}. \quad (12)$$

Holtz et al. [1992, 1995] experimentally examined the temperature and pressure dependence of H_2O solubility in a quasi-rhyolitic melt (composition 2 in Table 1) that is similar to natural rhyolitic melts in composition (Table 1). H_2O solubility in this melt is similar to that in rhyolitic melt of composition 1 in Table 1 (H. Behrens, personal communications, 1998) (Figure 7a). The model for H_2O solubility in this melt is derived as follows. It is assumed that K_2 in this melt is the same as that in rhyolitic melt (equation (10)) and is independent of H_2O_t to 14 wt % H_2O_t. That is, mixing of H_2O_m-OH-O species is assumed to be ideal for up to 14% H_2O_t. Although speciation is not well understood at such high H_2O_t, it is judged that using an approximate speciation model is better than simply assuming all dissolved H_2O_t dissociates into OH groups or ignoring speciation as in some previous models. For a given T and P ($= P_{H_2O}$), H_2O fugacity is calculated from the equation of state for H_2O [*Pitzer and Sterner*, 1994]. From every measured H_2O solubility, H_2O_m concentration can be calculated from K_2 and H_2O_t by combining (2), $[H_2O_m] + 0.5[OH] = [H_2O_t]$, and $[H_2O_m] + [OH] + [O] = 1$, leading to

$$[H_2O_m] = \frac{8X^2}{8X + K_2(1 - 2X) + [\{K_2(1 - 2X)\}^2 + 16K_2X(1 - X)]^{1/2}}, \quad (13)$$

where $X = [H_2O_t]$. Then $K_1 = [H_2O_m]/f_{H_2O}$ can be obtained for every solubility datum given by *Holtz et al*. [1992, 1995]. Table 4 lists how K_1 depends on T and P ($= P_{H_2O}$) for the AOQ melt. These data are used to calibrate the following equation by linear regression:

$$\ln K_1 = (-13.869 + 0.0002474P) + (3890.3 - 0.3948P)/T, \quad (14)$$

where P (total P, not necessarily P_{H_2O}) is in bars and T is in kelvins. Using (14) for K_1 and (10) for K_2, H_2O solubility can be calculated using (12) to an average 1σ accuracy of 0.19% H_2O_t in the range of 300–8000 bars and 700°–1350°C (Figures 7b and 7c) and a maximum error of 0.68% (at 700°C and 5000 bars).

To investigate whether the approach using the above formulation has extrapolative value, the model was also calibrated using only data with $P \leq 3$ kbar [*Holtz et al*., 1992, 1995], resulting in slightly different parameters from those in (14). The error in extrapolating such a model to 5 and 8 kbar is relatively small: At 5 kbar and 800°C the experimental solubility is 9.97% versus calculated 10.22% (12.72% if the *Moore et al*. [1998] model is used); at 8 kbar and 800°C the experimental solubility is 13.82% versus calculated 14.51% (23.15% using the

model of *Moore et al.* [1998]). This exercise shows that the solubility model incorporating speciation has extrapolative value.

The formulation in (14) also reproduces very well the H_2O solubility in rhyolitic melt (calculated curve 1 in Figure 7a), demonstrating its applicability to natural rhyolitic melts. Furthermore, the formulation also reproduces a datum for metastable H_2O solubility at 490°C and 250 bars in a rhyolitic glass (calculated 3.21% versus experimental ~3.1%, hydration data of *Zhang et al.* [1991a]), suggesting it can be extrapolated to low temperatures. Hence I recommend (10), (12), and (14) for the calculation of H_2O solubility from 0 to 8 kbar and from 500° to 1350°C (despite thermodynamic inconsistencies among the data discussed below). Figure 8 shows the calculated H_2O solubility as a function of P (= P_{H_2O}) at several temperatures and can be used for estimating H_2O solubility. Although accurate extension of this approach to examine the compositional dependence of H_2O solubility requires a knowledge of the speciation equilibrium in other melts, a rough estimate of speciation using (10) is better than simply ignoring the role of speciation.

Incorporation of more terms (such as terms linear to ln T, T, P^2/T, and $1/T^2$ to account for heat capacity, compressibility, etc.) into the expression of ln K_1 improves the quality of the fit only slightly, and the coefficients have large uncertainties. That is, incorporation of more terms can fit the data better at 700°–1350°C and

TABLE 4. Solubility of H_2O in the AOQ Melt

T, °C	P, bars	H_2O_t, wt %	f_{H_2O}, bars	$X_{H_2O_m}$	ln K_1
700	5000	10.07	3837	0.0979	−10.576
750	2000	6.00	1481	0.0476	−10.345
800	300	2.13	285.5	0.0096	−10.305
800	500	2.79	461.2	0.0146	−10.358
800	500	2.71	461.2	0.014	−10.403
800	500	2.91	461.2	0.0156	−10.293
800	700	3.77	626.2	0.0231	−10.206
800	700	3.74	626.2	0.0229	−10.218
800	1000	4.11	857.5	0.0263	−10.392
800	1000	4.07	857.5	0.0259	−10.407
800	1000	4.10	857.5	0.0262	−10.396
800	1300	5.02	1078	0.0351	−10.331
800	1400	5.16	1150	0.0365	−10.357
800	2000	5.86	1592	0.0437	−10.503
800	2000	5.84	1592	0.0435	−10.507
800	2000	5.77	1592	0.0428	−10.524
800	3000	7.45	2407	0.0608	−10.587
800	3000	7.45	2407	0.0608	−10.587
800	4000	8.94	3387	0.0774	−10.687
800	4800	9.38	4330	0.0824	−10.87
800	5000	9.90	4591	0.0883	−10.859
800	5000	10.07	4591	0.0903	−10.837
800	5000	9.86	4591	0.0879	−10.864
800	5000	10.02	4591	0.0897	−10.843
800	5000	10.04	4591	0.0899	−10.841
800	5000	9.94	4591	0.0888	−10.853
800	8000	13.95	10175	0.1356	−11.226
800	8000	13.70	10175	0.1327	−11.248
850	1000	4.00	889.4	0.0238	−10.53
850	2000	5.73	1687	0.0402	−10.644
850	5000	10.48	4919	0.0915	−10.893
900	500	2.72	476.7	0.0122	−10.57
900	500	2.48	476.7	0.0105	−10.72
900	2000	5.80	1769	0.0389	−10.724
950	2000	5.48	1838	0.0341	−10.894
1000	500	2.28	487.1	0.008	−11.014
1000	5000	10.65	5706	0.0841	−11.125
1050	2000	5.57	1947	0.0319	−11.019
1100	500	2.44	494.2	0.008	−11.033
1100	2000	5.31	1989	0.0284	−11.157
1100	5000	10.94	6080	0.082	−11.214
1100	5000	10.69	6080	0.0794	−11.246
1150	2000	5.47	2024	0.0285	−11.17
1150	2000	5.35	2024	0.0276	−11.205
1200	500	2.32	499.2	0.0066	−11.238
1200	1000	3.54	1000	0.0135	−11.211
1200	3000	7.25	3258	0.0424	−11.25
1200	4000	8.73	4676	0.0559	−11.335
1200	5000	10.85	6356	0.0765	−11.328
1350	1000	3.38	1019	0.011	−11.437

Three leftmost columns are from *Holtz et al.* [1992, 1995]; f_{H_2O} is calculated from *Pitzer and Sterner* [1994]; $X_{H_2O_m}$ is calculated using equation (13) and K_2 is calculated from equation (10). $K_1 = X_{H_2O_m}/f_{H_2O}$.

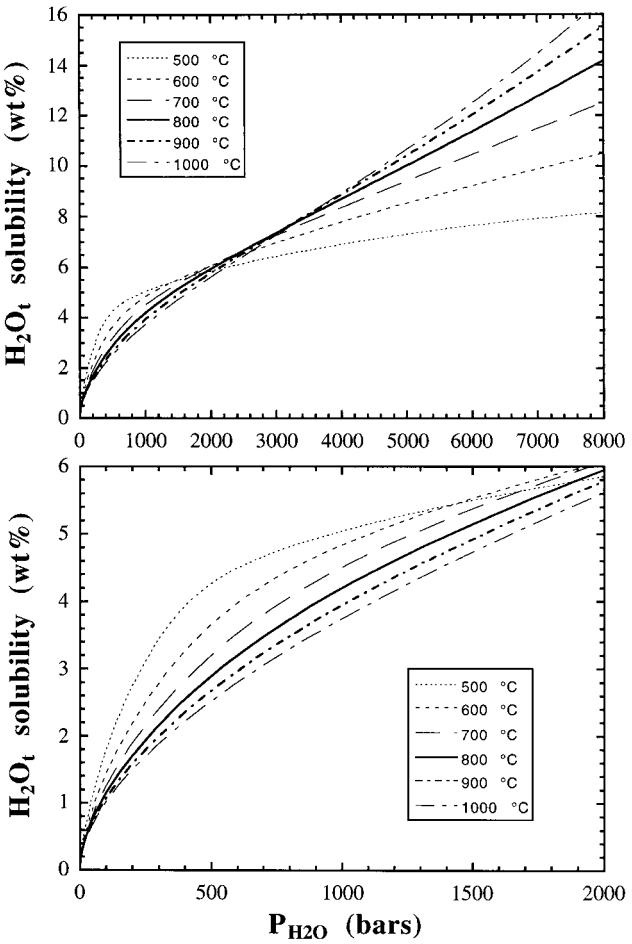

Figure 8. Calculated H_2O solubility in rhyolitic melts and metastable solubility in glasses using the solubility model in the present work, equation (12) with K_1 from equation (14) and K_2 from equation (10), for $P = P_{H_2O}$.

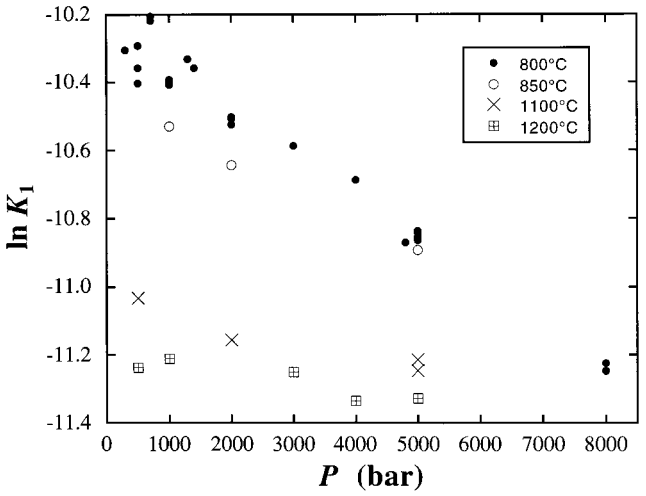

Figure 9. The plot of ln K_1 versus P at several fixed T. The absolute value of the slope at each given T is proportional to the partial molar volume of H_2O_m.

300–8000 bars but may cause difficulty in extrapolation. These other terms are not well-constrained by the solubility data at present and are not included.

4.3. An Inconsistency Between the Solubility Model and Partial Molar Volume Data

In principle, thermodynamic data may be derived from (14) and compared with those determined by independent methods to test the consistency and quality of all the data. For example, the partial molar volume of H_2O_m, $\bar{V}^{melt}_{H_2O_m}$, may be obtained as

$$\bar{V}^{melt}_{H_2O_m} = -RT\frac{\partial \ln K_1}{\partial P} = 32.8 - 0.02057T, \quad (15)$$

where T is in kelvins and $\bar{V}^{melt}_{H_2O_m}$ is in cm^3 mol^{-1}. The simplicity of the right-hand-side of (15) (e.g., there is no pressure term) clearly suggests that it is not possible yet to obtain accurate $\bar{V}^{melt}_{H_2O_m}$ from solubility data. Furthermore, $\bar{V}^{melt}_{H_2O_m}$ in (15) decreases with increasing T, an unreasonable result. $\bar{V}^{melt}_{H_2O_m}$ calculated from the above equation would be 15.9 cm^3 mol^{-1} at 550°C and 0 at 1321°C. The apparent decrease of $\bar{V}^{melt}_{H_2O_m}$ with T, although unexpected, is consistent with the ln K_1 versus P plot at several fixed T (Figure 9). The absolute values of the slope in ln K_1 versus P (which is proportional to $\bar{V}^{melt}_{H_2O_m}$) clearly decrease as T increases.

The term $\bar{V}^{melt}_{H_2O_t}$ has been determined from density measurements of silicate melts and glasses [*Ochs and Lange*, 1997, 1999]. For the purpose of comparison, $\bar{V}^{melt}_{H_2O_m}$ and $\bar{V}^{melt}_{H_2O_t}$ can be related as follows [*Zhang*, 1999]:

$$\bar{V}^{melt}_{H_2O_t} = \frac{X^{melt}_{H_2O_m}}{X^{melt}_{H_2O_t}}\bar{V}^{melt}_{H_2O_m} + \frac{X^{melt}_{(OH)_2-O}}{X^{melt}_{H_2O_t}}\bar{V}^{melt}_{(OH)_2-O}, \quad (16)$$

where the subscript $(OH)_2$-O means one cluster of two OH groups minus one oxygen, that is, H_2O dissolved in the form of OH groups. Because *Zhang* [1993] inferred from the speciation data that the partial molar volume of $(OH)_2$-O is only 0.7 cm^3 mol^{-1} greater than $\bar{V}^{melt}_{H_2O_m}$ at $P <$ 10 kbar, T = 550°C and H_2O_t = 0.8%, $\bar{V}^{melt}_{H_2O_t}$ is expected to be roughly the same as $\bar{V}^{melt}_{H_2O_m}$. However, the $\bar{V}^{melt}_{H_2O_m}$ values determined from solubility and speciation data are clearly different from $\bar{V}^{melt}_{H_2O_t}$ determined by *Ochs and Lange* [1997, 1999]. For example, at 850°C and ≤3 kbar, *Ochs and Lange* [1997, 1999] obtained $\bar{V}^{melt}_{H_2O_t}$ = 21 cm^3 mol^{-1}, whereas (15) gives $\bar{V}^{melt}_{H_2O_m}$ = 9.7 cm^3 mol^{-1}.

The inconsistency between solubility, speciation, and partial molar volume data can also be examined from a different approach. At a constant temperature, K_1 depends on pressure as follows:

$$K_1 = A_1 \exp\left[-\int_1^P \bar{V}^{melt}_{H_2O_m}\, dP/(RT)\right], \quad (17)$$

where P is in bars. Using $\bar{V}^{melt}_{H_2O_m} \approx \bar{V}^{melt}_{H_2O_t}$ = 21 cm^3 mol^{-1} in albitic melt at 850°C below 3 kbar [*Ochs and Lange*, 1997, 1999] and K_2 = 0.410 at 850°C in rhyolitic melt (equation (10)), H_2O solubility can be calculated from (12) given T and P if A_1 is specified. In other words, the above formulation can be used to fit the solubility data to obtain A_1. Such a best fit solubility curve at 850°C is shown as curve 2 in Figure 7a. Though the agreement is not bad, the shape of the calculated curve does not match the data in detail so that either the high-pressure or low-pressure data cannot be well fit. (If K_2 is chosen to be 0.99 from *Nowak and Behrens* [1995], the fit, shown as curve 3 in Figure 7a, is slightly worse.) The imperfect fit indicates that there is some inconsistency between the speciation model, the solubility, and partial molar volume data. The examination also shows high precision and accuracy is necessary if $\bar{V}^{melt}_{H_2O_m}$ is to be derived from solubility data.

The inconsistency between solubility, speciation, and partial molar volume data may be explained in several different ways. (1) $\bar{V}^{melt}_{H_2O_t}$ determined from density data by linear regression may be in error. Although density measurements have very high accuracy, obtaining the partial molar volume by assuming all $\bar{V}$ are constant may generate errors. (2) The inability to accurately constrain higher-order terms using the solubility data means that $\bar{V}^{melt}_{H_2O_m}$ (and similarly $\Delta\bar{H}^0_{r1}$) may not be well-constrained at present. (3) The most likely explanation is as follows: The H_2O solubility in AOQ melt is determined at 700°–1350°C and has its best precision at high H_2O_t (and hence high P) because Karl-Fischer titration is used to obtain H_2O_t, whereas the H_2O speciation in rhyolitic glasses is determined at 400°–600°C and the speciation model is calibrated only at ≤2.4% H_2O_t. Combination of the two data sets to model solubility requires the extrapolation of the speciation model to much higher T and much higher H_2O_t, which may be problematic and result in inaccuracy of $\bar{V}^{melt}_{H_2O_m}$. Whatever the explanations, more work is necessary to maintain data consistency. With future improvement on these experimental data, an op-

timization method can be used to reconcile and constrain all the input data.

An alternative approach to model H_2O solubility and to extract K_2 at high H_2O_t is to assume that the partial molar volume data [*Ochs and Lange*, 1997, 1999] are accurate and applicable. If low-pressure solubilities are well known, then K_1 at low pressures can be calculated from the solubility data and K_2 (since K_2 is well known at $\leq$2.4% H_2O_t). K_1 as a function of pressure can then be obtained from (17). From high-pressure solubility data, K_2 at high pressures, i.e., at high H_2O_t, can be obtained. Using the dependence of K_2 on H_2O_t, an expression for calculation of solubility can be obtained. This approach requires accurate solubility data at low pressures and various T, which are not available at present.

5. DIFFUSION OF H_2O IN RHYOLITIC GLASSES AND MELTS

Diffusion of H_2O in rhyolitic and other melt plays a critical role in bubble growth. Diffusion is caused by random motion of molecules, atoms, and ions in a phase. Although such random motion is always present with or without a concentration gradient, only when there is a concentration (more accurately a chemical potential) gradient does diffusion lead to a net mass flux. For one-dimensional binary diffusion the mass flux **J** can be written as [e.g., *Crank*, 1975]

$$\mathbf{J} = -D\frac{\partial C}{\partial x}, \tag{18}$$

where D is the binary diffusivity, C is the concentration of the diffusing component, x is distance, and $\partial C/\partial x$ is the concentration gradient. The concentration variation with time can be written as

$$\frac{\partial C}{\partial t} = -\frac{\partial \mathbf{J}}{\partial x} = \frac{\partial}{\partial x}\left(D\frac{\partial C}{\partial x}\right). \tag{19}$$

H_2O diffusion in commercial glasses has been investigated extensively (see *Doremus* [1994] for a review). I concentrate on H_2O diffusion in rhyolitic and quasi-rhyolitic glasses and melts.

Shaw [1974] carried out the first study of H_2O diffusion in a rhyolitic melt. He showed that the diffusivity of the H_2O component is high compared with that of other components and increases with its concentration. Subsequent reports [*Friedman and Long*, 1976; *Jambon*, 1979; *Delaney and Karsten*, 1981; *Karsten et al*., 1982; *Lapham et al*., 1984] confirmed the conclusions and also showed that the activation energy for H_2O diffusion is low. These workers used (19) or a variation of it to obtain the diffusivity of the H_2O component.

5.1. Role of Speciation During H_2O Diffusion at Low H_2O_t

Because the dissolved H_2O component is present in silicate melts and glasses as at least two species, H_2O_m molecules and OH groups, and because H_2O_m and OH are expected to have different diffusivities, it is natural to consider the role of speciation in diffusion. This approach started from glass scientists for treating H_2O diffusion at low H_2O_t [e.g., *Doremus*, 1969, 1994]. *Wasserburg* [1988] presented a formal analysis on how to treat the diffusion of the H_2O component at low to high H_2O_t if H_2O_m is the diffusing species. *Zhang et al*. [1991a] carried out experiments and examined the role of speciation in the diffusion of the H_2O component in a rhyolitic glass/melt containing 0.4–1.8% H_2O_t at 1 bar and 400°–550°C. They treat the one-dimensional diffusion of the H_2O component by explicitly considering the role of speciation:

$$\frac{\partial[H_2O_t]}{\partial t} = \frac{\partial}{\partial x}\left\{D_{H_2O_m}\frac{\partial[H_2O_m]}{\partial x} + D_{OH}\frac{\partial[OH]/2}{\partial x}\right\}, \tag{20}$$

where $D_{H_2O_m}$ is the diffusivity of molecular H_2O and D_{OH} is the diffusivity of OH groups. From diffusion experiments, H_2O_t, H_2O_m, and OH profiles are measured. Hence both $D_{H_2O_m}$ and D_{OH} can be obtained by fitting the profiles to the above equation if the diffusivities are assumed to be constant. Whether they are indeed constant can be determined from the quality of the fit. Using this approach, *Zhang et al*. [1991a] found that their H_2O diffusion data can be almost perfectly modeled if (1) the $D_{OH}/D_{H_2O_m}$ ratio is much smaller than 1, and (2) $D_{H_2O_m}$ is roughly constant over the H_2O_t range of each experiment (<2%). That is, of the two species of the dissolved H_2O component, only molecular H_2O_m is mobile, whereas OH is immobile. The OH profile is not due to diffusion of OH, but due to the local interconversion between H_2O_m and OH. *Zhang et al*. [1991a] obtained $D_{H_2O_m}$ values from diffusion profiles, in which the species concentrations were calculated using the calibration of *Newman et al*. [1986].

There are other systems in which mobile and immobile "species" are inferred but cannot be directly measured. Therefore a detailed understanding of the role of H_2O_m and OH in H_2O diffusion, where both can be measured (even with the complexities discussed earlier), may be instructive for these systems in which mobile and immobile species are not directly measurable [e.g., *Wang et al*., 1996]. *Zhang and Stolper* [1991] investigated diffusion of the H_2O component in basaltic melt with 0.04–0.4% H_2O_t at 10 kbar and 1300°–1500°C. They found that $D^*_{H_2O_t}$ in a basaltic melt is significantly higher than in a rhyolitic melt at similar temperatures. Although the H_2O_m concentration cannot be directly measured, the observed proportionality between $D^*_{H_2O_t}$ and H_2O_t led them to suggest that molecular H_2O_m is also the diffusing species.

5.2. Distinguishing Different Diffusivities of H_2O Diffusion

Because of the presence of two species, the diffusion of the H_2O component is complicated. *Zhang et al*. [1991b] examined the general role of speciation in diffusion and the particular case of how H_2O diffusion affects the hydrothermal oxygen "self-diffusion." The strong dependence of H_2O diffusivity on H_2O_t also leads to differences in several definitions of diffusivities that are typically identical. For example, diffusion-out and diffusion-in diffusivities obtained from mass loss and gain methods assuming constant D are typically the same. However, for H_2O diffusion, diffusion-out (dehydration) and diffusion-in (hydration) diffusivities are different. In this section the different diffusivities and how they are related are summarized [*Zhang et al*., 1991a, b; *Wang et al*., 1996].

1. Diffusivity of molecular H_2O_m ($D_{H_2O_m}$) is defined in (20) and obtainable by fitting diffusion profiles to the equation. Its dependence on H_2O_t is weak at $H_2O_t \leq 2.0\%$ [*Zhang et al*. [1991a] and the present work). However, at $>2\%$ H_2O_t, $D_{H_2O_m}$ increases rapidly (exponentially) with H_2O_t [*Zhang and Behrens*, 1998b, submitted manuscript, 1999].

2. Diffusivity of OH groups (D_{OH}) is defined in (20) and is much smaller than $D_{H_2O_m}$ at $H_2O_t < 2.0\%$ [*Zhang et al*., 1991a].

3. Diffusivity of the H_2O component ($D^*_{H_2O_t}$) is defined in (19). The diffusivity of each species reflects the intrinsic mobility of the species, but $D^*_{H_2O_t}$ does not. Hence $D^*_{H_2O_t}$ is also called the effective or apparent diffusivity of total H_2O, or simply the diffusivity of H_2O_t. Because it depends strongly on H_2O_t, it is often obtained using the Boltzmann-Matano method [*Nowak and Behrens*, 1997; *Behrens and Nowak*, 1997], or by fitting concentration profiles assuming $D^*_{H_2O_t} \propto [H_2O_t]$ at low H_2O_t or by assuming a function for $D_{H_2O_m}$ [*Zhang et al*., 1991a; *Zhang and Behrens*, 1998b, submitted manuscript, 1999]. $D^*_{H_2O_t}$ can be calculated from species diffusivities using

$$D^*_{H_2O_t} = D_{H_2O_m} \frac{d[H_2O_m]}{d[H_2O_t]} + D_{OH} \frac{d[OH]/2}{d[H_2O_t]}. \quad (21)$$

If H_2O_m is the diffusing species, then

$$D^*_{H_2O_t} = D_{H_2O_m} \frac{d[H_2O_m]}{d[H_2O_t]}. \quad (22)$$

The above equation allows the calculation of $D^*_{H_2O_t}$ if $D_{H_2O_m}$ is known and the differential $d[H_2O_m]/d[H_2O_t]$ can be calculated. If equilibrium is reached, the differential can be calculated from a speciation model. Different diffusivities (such as $D^*_{H_2O_t}$ and $D_{H_2O_m}$) may have different temperature dependence [*Zhang et al*., 1991a].

4. Diffusion-out diffusivity ($\bar{D}^*_{out}$) is defined by [e.g., *Crank*, 1975; *Wang et al*., 1996]

$$M_t = M_0 - M_0 \sqrt{\frac{16\overline{D^*_{out}}}{\pi L^2}} \sqrt{t}, \quad (23)$$

where M_t is the total H_2O_t mass still remaining in a slab after partial dehydration (desorption), M_0 is the initial mass, and L is the thickness of the slab. The above equation is valid when M_t/M_0 is greater than 0.5 and when the surface concentration of H_2O_t is zero. The $\bar{D}^*_{out}$ is some kind of average of $D^*_{H_2O_t}$ across the whole diffusion profile. At low H_2O_t ($\leq 2\%$), $D^*_{H_2O_t} \propto [H_2O_t]$, leading to

$$\bar{D}^*_{out} = 0.347 D^*_{H_2O_t,0}, \quad (24)$$

for zero surface H_2O_t, where $D^*_{H_2O_t,0}$ is $D^*_{H_2O_t}$ at the initial H_2O_t.

5. Diffusion-in diffusivity ($\bar{D}^*_{in}$) is defined by [e.g., *Crank*, 1975]

$$M_t = M_0 + M_1 \sqrt{\frac{16\overline{D^*_{in}}}{\pi L^2}} \sqrt{t}, \quad (25)$$

where L is the thickness of the slab, M_t is the total H_2O_t mass that is now in the slab after partial hydration (sorption), M_0 is the initial mass, and M_1 is the total mass that would enter the slab after infinite time. The above equation is valid when $(M_t - M_0)/M_1$ is less than 0.5. The $\bar{D}^*_{in}$ is another average of $D^*_{H_2O_t}$ across the whole diffusion profile. If D is independent of concentration, $\bar{D}^*_{in} = \bar{D}^*_{out} = D$. However, for H_2O diffusion, $\bar{D}^*_{in} \neq \bar{D}^*_{out} \neq D^*_{H_2O_t} \neq D_{H_2O_m}$. At low H_2O_t ($\leq 2\%$), $D^*_{H_2O_t} \propto [H_2O_t]$, leading to

$$\bar{D}^*_{in} = 0.619 D^*_{H_2O_t,s}, \quad (26)$$

for zero initial H_2O_t where $D^*_{H_2O_t,s}$ is $D^*_{H_2O_t}$ at the surface H_2O_t.

6. The D-H interdiffusion coefficient ($D_{D\text{-}H}$) is obtained from (19) by allowing D_2O to diffuse in (or out) of a hydrous glass/melt by maintaining constant mole fractions (not weight percent) of $D_2O_t + H_2O_t$. Since the total $D_2O_t + H_2O_t$ is constant, the $D_{D\text{-}H}$ is constant in an experiment and can be obtained by fitting an error function to the diffusion profile. However, $D_{D\text{-}H}$ depends on $[D_2O_t] + [H_2O_t]$. If molecular D_2O_m and H_2O_m are the diffusing species, then

$$D_{D\text{-}H} = 0.5 D^*_{H_2O_t}. \quad (27)$$

If OH and OD are the diffusing species, then

$$D_{D\text{-}H} = D^*_{H_2O_t}. \quad (28)$$

Equations (27) and (28) show that accurate determination of $D_{D\text{-}H}$ and $D^*_{H_2O_t}$ can be used to distinguish the diffusing species. Equation (27) also shows that isotopic exchange can be slower than chemical diffusion of a component. This result is interesting because *Lesher* [1990, 1994] and *van der Laan et al*. [1994] showed that homogenization of isotopic ratio gradients of K, Ca, Sr, and Nd is typically more rapid than or at about the same rate as that of chemical concentration gradients.

5.3. H_2O Diffusion at High H_2O_t: Controversy and Discussion

In light of recent progress, the calibration and speciation used by *Zhang et al*. [1991a] in extracting $D_{H_2O_m}$ are not accurate anymore. Hence $D_{H_2O_m}$ values are inaccurate. Nevertheless, because the total H_2O diffusivity ($D^*_{H_2O_t}$) is constrained from experimental diffusion profiles, it is independent of the specific speciation model and $D_{H_2O_m}$. Therefore $D^*_{H_2O_t}$ can still be retrieved accurately from (22) from both $D_{H_2O_m}$ and the speciation model of *Zhang et al*. [1991a] as long as self-consistency is maintained. However, one cannot combine $D_{H_2O_m}$ of *Zhang et al*. [1991a] and a new, even a more accurate, speciation model (such as equation (10) above) to calculate $D^*_{H_2O_t}$, unless H_2O_m and OH concentrations and $D_{H_2O_m}$ are recalculated using the new calibration.

Recently, *Nowak and Behrens* [1997] and *Behrens and Nowak* [1997] reported important new diffusion data in the AOQ (Table 1) melt with 0–9% H_2O_t at 0.5–5 kbar and 800°–1200°C. *Nowak and Behrens* [1997] found a very strong dependence of $D^*_{H_2O_t}$ on H_2O_t, especially at $H_2O_t > 3\%$, which differs from the model of *Zhang et al*. [1991a]. Furthermore, they found that $D^*_{H_2O_t}$ decreases with increasing pressure. They fit their experimental diffusivity data as a linear function of T, P/T, and a polynomial function of H_2O_t. *Behrens and Nowak* [1997] examined the dependence of H_2O_t diffusivity on the anhydrous composition of polymerized melts and found that H_2O_t diffusivity does not change significantly from albitic to rhyolitic melt.

In order to examine whether the formulation of *Zhang et al*. [1991a] applies to high T and low H_2O_t, *Behrens and Nowak* [1997] compared $D^*_{H_2O_t}$ values from their experiments with those calculated (and extrapolated) from *Zhang et al*. [1991a]. They calculated $D^*_{H_2O_t}$ by adopting the formulation for $D_{H_2O_m}$ of *Zhang et al*. [1991a] but using their own in situ speciation model [*Nowak and Behrens*, 1995]. They found disagreement in this comparison. Further, they calculated $D^*_{H_2O_t}$ at low 490°C and 0.5% H_2O_t using their own equation [*Nowak and Behrens*, 1997] and found that the value is significantly different from the experimental value of *Zhang et al*. [1991a]. From these disagreements they concluded that the formulation of *Zhang et al*. [1991a] cannot be extrapolated to high temperature and that their own expression cannot be extrapolated to low temperature, possibly owing to the effect of glass transition. When they compared the shape of the $D^*_{H_2O_t}$ versus H_2O_t curve, they found that the calculated curve using *Zhang et al*. [1991a] does not increase rapidly enough as H_2O_t increases, especially at $H_2O_t > 3\%$. From this disagreement they concluded that the formulation of *Zhang et al*. [1991a] cannot predict their experimental $D^*_{H_2O_t}$ at high H_2O_t.

Because *Behrens and Nowak* [1997] combined the speciation model of *Nowak and Behrens* [1995] and the $D_{H_2O_m}$ expression of *Zhang et al*. [1991a], their calculation of $D^*_{H_2O_t}$ using the formulation of Zhang et al. is not self-consistent. In Figure 10 I compare experimental $D^*_{H_2O_t}$ values of *Nowak and Behrens* [1997] and *Behrens and Nowak* [1997] with those calculated from *Zhang et al*. [1991a]. In Figure 10a, all the experimental data of *Nowak and Behrens* [1997] and *Behrens and Nowak* [1997] on AOQ melt and albitic melt at $H_2O_t < 2.0\%$, $P \leq 1$ kbar are compared with calculated $D^*_{H_2O_t}$ using the formulation of *Zhang et al*. [1991a]. The agreement is excellent, demonstrating that the formulation of *Zhang et al*. [1991a] can be used to predict diffusivities at high T and that the effect of glass transition is small. That is, one of the conclusions by *Behrens and Nowak*

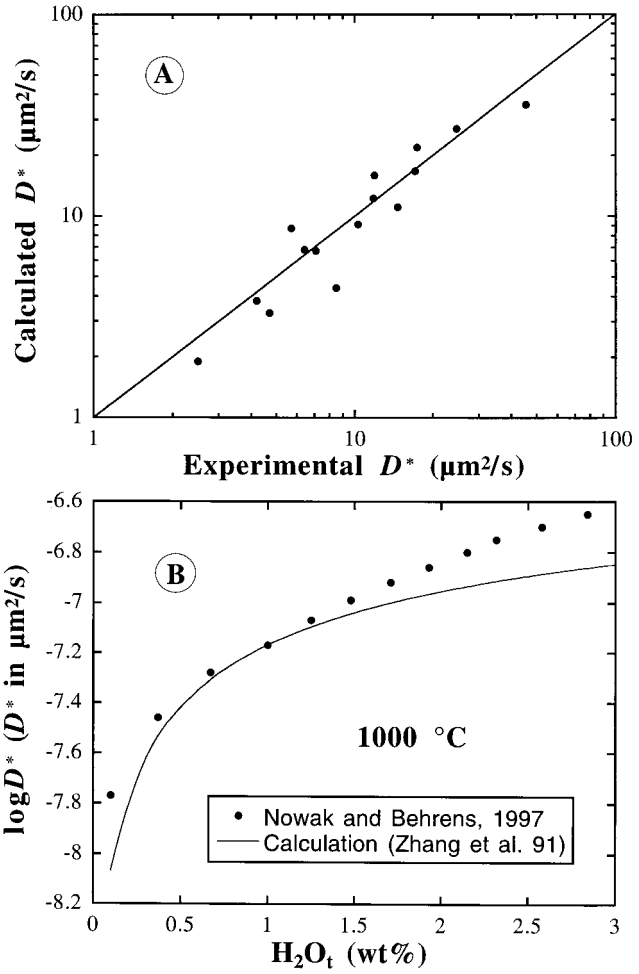

Figure 10. (a) Comparison of all experimental $D^*_{H_2O_t}$ (horizontal axis) at 0.5–2.0% H_2O_t, 900°–1150°C, and 500–1000 bars [*Nowak and Behrens*, 1997; *Behrens and Nowak*, 1997] with $D^*_{H_2O_t}$ calculated using the formulation of *Zhang et al*. [1991a]. Higher-pressure data are not used in the comparison because $D^*_{H_2O_t}$ depends on pressure [*Nowak and Behrens*, 1997]. The solid line is the 1:1 line. (b) Experimental $D^*_{H_2O_t}$ versus H_2O_t (points) on AOQ melt at 1000°C and 1 kbar [*Nowak and Behrens*, 1997, Figure 7] compared with calculated $D^*_{H_2O_t}$ using $D_{H_2O_m}$ and the speciation model of *Zhang et al*. [1991a] (solid curve). The deviation at 0.1% H_2O_t is almost certainly because of errors in the $D^*_{H_2O_t}$ value of *Nowak and Behrens* [1997]. The deviation at higher H_2O_t means that the model of *Zhang et al*. [1991a] cannot be extrapolated to high H_2O_t.

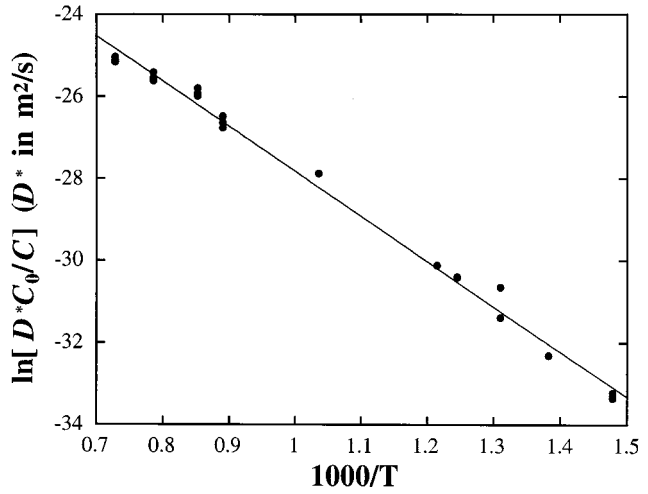

Figure 11. The value of ln $[D^*_{H_2O_t} C_0/C]$ versus $1/T$, where C is the mass fraction (or weight percent) of H_2O_t and C_0 is the reference concentration chosen to be the mass fraction of 0.01 (i.e., 1 wt %). That is, $D^*_{H_2O_t} C_0/C$ is $D^*_{H_2O_t}$ at 1% H_2O_t. Data are from *Lapham et al.* [1984], *Zhang et al.* [1991a], *Wang et al.* [1996], and *Nowak and Behrens* [1997]. The solid line is a straight-line fit through the data.

[1997] is incorrect. This result lends support to the model of *Zhang et al.* [1991a] that H_2O_m is the diffusing species for the diffusion of the H_2O component and $D_{H_2O_m}$ is roughly independent of H_2O_t at 400°–1200°C and $H_2O_t \leq 2\%$. The inaccuracy in extrapolating their own diffusivity expression to lower T [*Nowak and Behrens*, 1997; *Behrens and Nowak*, 1997] is probably due to the use of a polynomial function.

In Figure 10b the experimental data at a single T and P but variable H_2O_t are compared with calculations. It can be seen that although the agreement at $\leq 2\%$ H_2O_t is very good, the shape of the $D^*_{H_2O_t}$ versus H_2O_t curve based on experimental data is clearly different from that of the calculated. At high H_2O_t the calculation based on the work of *Zhang et al.* [1991a] yields a $D^*_{H_2O_t}$ that is lower than the experimental data, showing that the formulation of *Zhang et al.* [1991a] cannot be used to predict $D^*_{H_2O_t}$ at high H_2O_t. Hence one of the main conclusions of *Behrens and Nowak* [1997] is correct. This conclusion is based primarily on the shape of the $D^*_{H_2O_t}$ versus H_2O_t curve and is hence less dependent on the exact $D^*_{H_2O_t}$ values.

The mechanism for the rapid increase of $D^*_{H_2O_t}$ with H_2O_t at high H_2O_t is not clear. It may result from an increase of $D_{H_2O_m}$ with H_2O_t [*Zhang and Behrens*, 1998b, submitted manuscript, 1999] or from a significant contribution of OH to the diffusion, or some other mechanisms (such as the formation of OH pairs proposed by *Behrens and Nowak* [1997]). Because preeruptive melts of explosive volcanic eruptions often contain 6% or more H_2O_t, it is crucial to quantify the diffusivity of H_2O_t at both low and high H_2O_t for the quantitative modeling of bubble growth. *Zhang and Behrens* [1998b, submitted manuscript, 1999] are carrying out a comprehensive investigation of H_2O diffusion as a function of H_2O_t, T, and P.

5.4. A Simple Formula for H_2O Diffusion at Low H_2O_t and 400°–1100°C

Because the formulation of *Zhang et al.* [1991a] is difficult to use and because calibration of the infrared technique is still improving, I present a simple equation below for calculating $D^*_{H_2O_t}$ at $H_2O_t \leq 2\%$ for ease of use. The formulation of *Zhang et al.* [1991a] implies that at low H_2O_t, $D^*_{H_2O_t}$ is proportional to H_2O_t if local species equilibrium is maintained. *Nowak and Behrens* [1997] also showed that $D^*_{H_2O_t}$ is proportional to H_2O_t at $H_2O_t \leq 2\%$ at high T. Hence diffusivity data are used to fit

$$D^*_{H_2O_t} = \frac{C_0}{C} \exp\left(A - \frac{E_a}{RT}\right), \quad (29)$$

where A is a constant, C is mass fraction of H_2O_t, C_0 is the reference mass fraction of H_2O_t, chosen to be 0.01 (i.e., 1%), and E_a is the effective activation energy (in J mol^{-1} K^{-1}) for H_2O_t diffusion. Figure 11 shows $D^*_{H_2O_t}$ data at $H_2O_t \leq 2\%$; $D^*_{H_2O_t}$ at 400°–550°C calculated from $D_{H_2O_m}$ data of *Zhang et al.* [1991a] assuming local species equilibrium, $D^*_{H_2O_t}$ at 697°C of *Wang et al.* [1996], $D^*_{H_2O_t}$ at 850°C from *Lapham et al.* [1984] with refit of *Zhang et al.* [1991a], and 0.5- to 1-kbar data of *Nowak and Behrens* [1997]. A small adjustment was made to the $D^*_{H_2O_t}$ at 0.5–1 kbar using an activation volume of 9 cm^3 mol^{-1} [*Nowak and Behrens*, 1997]. All these 1-bar $D^*_{H_2O_t}$ values (400°–1100°C) are shown in Figure 11. Although the data seem to show a small curvature in ln $[D^*_{H_2O_t} C_0/C]$ versus $1/T$, the curvature is small and only slightly outside the experimental uncertainties. Therefore the effect of glass transition on the H_2O diffusion behavior is negligible [*Zhang et al.*, 1991a; *Watson*, 1994]. A simple straight line is used to fit the data, yielding

$$D^*_{H_2O_t} = (C/C_0) \exp[-16.83 - 10992/T], \quad (30)$$

where T is in kelvins and $D^*_{H_2O_t}$ is in m^2 s^{-1}. The above equation is applicable to 400°–1200°C, 0–2% H_2O_t, and 1 bar. The average (1σ) and maximum error in using the above equation to predict ln $D^*_{H_2O_t}$ is 0.24 and 0.60. $D^*_{H_2O_t}$ at higher H_2O_t and 800°–1200°C can be calculated using the formulation of *Nowak and Behrens* [1997]. Work is under way on a general equation to predict $D^*_{H_2O_t}$ at both low and high H_2O_t [see *Zhang and Behrens*, 1998b, submitted manuscript, 1999]. The main advantage of the above simple equation is its ease of use. However, it does not have the generality of the formulation of *Zhang et al.* [1991a] in that it cannot handle local disequilibrium, which may be important at low T (<550°C) and low H_2O_t (<0.3%).

6. CONCLUSIONS AND FUTURE DIRECTIONS

Major progress has been made on H_2O in silicate melts and glasses in the last 5 years, although there has

been confusion. I hope that the above review clarifies some of the confusion and controversies. There are still many unsolved issues. The following is a summary of our present understanding on several issues concerning H_2O in rhyolitic glasses and melts.

1. Despite extensive research, more work is still necessary for accurate calibration of the infrared technique for room temperature measurement of H_2O. The calibration is complicated because molar absorptivities depend on both H_2O_t content and the measurement temperature. Specifically, improvement is necessary for measurement of species concentrations at $H_2O_t > 2.7\%$ and for H_2O_t determination both below 0.2% and above 5%. Furthermore, interlaboratory comparison of bulk H_2O analyses between manometry and Karl-Fischer titration will be helpful. Besides room temperature calibrations, calibration for in situ high-temperature measurements is also much needed.

2. In studying the equilibrium of the homogeneous reaction $H_2O_m + O \Leftrightarrow 2OH$ in rhyolitic melt and glass, experimental data using the quench technique are almost certainly valid as long as the experimental temperature is low enough (typically 400°–600°C) for the speciation to be quenched. The interpretation of the in situ speciation data, on the other hand, must await the quantification of the temperature effect on molar absorptivities. On the basis of quenched speciation data up to 2.4% H_2O_t, and using the most recent calibration, the equilibrium constant for the species reaction in rhyolitic melt and glass is independent of H_2O_t and can be expressed as [*Zhang et al*., 1997a]

$$K_2 = [OH]^2/\{[H_2O_m][O]\} = 6.53e^{-3110/T}.$$

Better room temperature calibration at higher H_2O_t, in situ high-temperature calibration and in situ investigation of species equilibrium will allow improvement of the above speciation model.

3. Many previous solubility models (including the recent model of *Moore et al*. [1998]) do not account for H_2O speciation in silicate melts. They are therefore very useful for interpolation but not useful for extrapolation. Using the recent speciation model, an updated solubility model has been developed using the solubility data of *Holtz et al*. [1992, 1995], leading to the following expression for the equilibrium constant for the heterogeneous reaction H_2O (vapor) $\Leftrightarrow$ H_2O_m (melt):

$$K_1 = [H_2O_m]/f_{H_2O} = \exp[(-13.869 + 0.0002474P) + (3890.3 - 0.3948P)/T].$$

The solubility of the H_2O component at 800°–1350°C and 0–8000 bars can be calculated using

$$[H_2O_t] = [H_2O_m] + 0.5[OH] = K_1 f + \frac{K_1K_2f(1 - K_1f)}{K_1K_2f + [(K_1K_2f)^2 + 4K_1K_2f(1 - K_1f)]^{1/2}},$$

where f is the fugacity of H_2O and K_1 and K_2 are given above. The accuracy of the above equation approaches the analytical accuracy (1σ accuracy of 0.19 wt % H_2O_t). The above expressions may be extrapolated to 500°C. Future experimental investigation of H_2O solubility at both high pressure (>3 kbar) and low pressure (<100 bars) and as a function of temperature will be important to further constrain the solubility model and mechanism.

4. At $H_2O_t \leq 2\%$ the H_2O diffusion model of *Zhang et al*. [1991a] can be used to accurately (meaning with an average accuracy of 30% relative) calculate $D^*_{H_2O_t}$ in rhyolitic melt from 400°C to 1200°C. Glass transition does not significantly affect the diffusion behavior. A simple equation for the calculation of H_2O_t diffusivity (in $m^2\ s^{-1}$) is

$$D^*_{H_2O_t} = (C/C_0)\exp[-16.83 - 10992/T],$$

where T is in kelvins, C is H_2O_t content, C_0 is the reference concentration of 1 wt % H_2O_t, and $D^*_{H_2O_t}$ is in $m^2\ s^{-1}$. The above expression is applicable to 400°–1200°C, 1 bar, and ≤2% H_2O_t. At $H_2O_t > 2\%$, neither the formulation of *Zhang et al*. [1991a] nor the above equation is applicable. The work of *Nowak and Behrens* [1997] and *Behrens and Nowak* [1997] significantly expanded the database on H_2O diffusion. Their H_2O diffusivity expressions are applicable at $H_2O_t > 1\%$ and ≥800°C. Because *Nowak and Behrens* [1997] used a polynomial to fit their experimental diffusivity data, their expression may not extrapolate well. Future experimental study is necessary for formulating a general model to encompass H_2O diffusion at both low and high H_2O_t and as a function of T and P and for understanding the diffusion mechanism of the H_2O component at higher H_2O_t.

Improvement on the above issues will not only constrain the above issues, but also will impact on our understanding of volcanic eruptions, the thermodynamics, transport, and other physical and chemical properties of hydrous magma, and glass durability.

ACKNOWLEDGMENTS. The first draft of this paper (presented at the Geological Conference for the Centennial Celebration of Peking University) was started in 1997 and finished in early 1998 while I was visiting the Institut für Mineralogie, Universität Hannover, Germany. I thank H. Behrens for his hospitality during my visit. Many thanks to H. Behrens, E. J. Essene, F. Holtz, R. A. Lange, M. Nowak, A. Withers, and Z. Xu for informal reviews and stimulating discussion and to my students and coworkers over the last 10 years. Detailed and constructive reviews by B. de Jong, M. C. Wilding, and P. deMenocal are appreciated. This work is partially supported by NSF grants EAR-9458368 and EAR-9706107.

Roel Snieder was the Editor responsible for this paper. He thanks Bernard de Jong and Martin C. Wilding for the technical reviews and Peter B. deMenocal for the cross-disciplinary review.

REFERENCES

Anderson, A. T., S. Newman, S. N. Williams, T. H. Druitt, C. Skirius, and E. Stolper, H_2O, CO_2, Cl and gas in Plinian and ash-flow Bishop rhyolite, *Geology*, *17*, 221–225, 1989.

Bagdassarov, N. S., D. B. Dingwell, and M. C. Wilding, Rhyolite magma degassing: An experimental study of melt vesiculation, *Bull. Volcanol*., *57*, 587–601, 1996.

Behrens, H., Determination of water solubilities in high-viscosity melts: An experimental study on $NaAlSi_3O_8$ and $KAlSi_3O_8$ melts, *Eur. J. Mineral*., *7*, 905–920, 1995.

Behrens, H., and M. Nowak, The mechanisms of water diffusion in polymerized silicate melts, *Contrib. Mineral. Petrol*., *126*, 377–385, 1997.

Behrens, H., C. Romano, M. Nowak, F. Holtz, and D. B. Dingwell, Near-infrared spectroscopic determination of water species in glasses of the system $MAlSi_3O_8$ (M = Li, Na, K): An interlaboratory study, *Chem. Geol*., *128*, 41–63, 1996.

Behrens, H., A. Withers, and Y. Zhang, In situ IR spectroscopy on hydrous albitic and rhyolitic glasses and its implications for water speciation and water reactions in silicate glasses and melts, *Mineral Mag*., *62A*, 139–140, 1998.

Blank, J. G., E. M. Stolper, and M. R. Carroll, Solubilities of carbon dioxide and water in rhyolitic melt at 850°C and 750 bars, *Earth Planet. Sci. Lett*., *119*, 27–36, 1993.

Burnham, C. W., Hydrothermal fluids at the magmatic stage, in *Geochemistry of Hydrothermal Ore Deposits*, edited by H. L. Barnes, pp. 34–76, Holt, Rinehart, and Winston, Austin, Tex., 1967.

Burnham, C. W., Water and magmas: A mixing model, *Geochim. Cosmochim. Acta*, *39*, 1077–1084, 1975.

Burnham, C. W., Development of the Burnham model for prediction of H_2O solubility in magmas, *Rev. Mineral*., *30*, 123–129, 1994.

Burnham, C. W., and N. F. Davis, The role of H_2O in silicate melts, II, Thermodynamic and phase relations in the system $NaAlSi_3O_8$-H_2O to 10 kilobars, 700° to 1100°C, *Am. J. Sci*., *274*, 902–904, 1974.

Carroll, M. R., and J. R. Holloway (Eds.), *Volatiles in Magmas*, *Rev. Mineral*., *30*, 517 pp., Mineralogical Society of America, Washington, DC, 1994.

Crank, J., *The Mathematics of Diffusion*, 414 pp., Clarendon, Oxford, England, 1975.

Danyushevsky, L. V., T. J. Falloon, A. V. Sobolev, A. J. Crawford, M. Carroll, and R. C. Price, The H_2O content of basaltic glasses from southwest Pacific back-arc basins, *Earth Planet. Sci. Lett*., *117*, 347–362, 1993.

Davis, K. M., and M. Tomozawa, An infrared spectroscopic study of water-related species in silica glasses, *J. Non Cryst. Solids*, *201*, 177–198, 1996.

De Jong, B. H. W. S., J. van Hoek, W. S. Veeman, and D. V. Manson, X-ray diffraction and 29Si magic-angle-spinning NMR of opals: Incoherent long- and short-range order in opal-CT, *Am. Mineral*., *72*, 1195–1203, 1987.

Delaney, J. R., and J. L. Karsten, Ion microprobe studies of water in silicate melts: Concentration-dependent water diffusion in obsidian, *Earth Planet. Sci. Lett*., *52*, 192–202, 1981.

Dingwell, D. B., and S. L. Webb, Relaxation in silicate melts, *Eur. J. Mineral*., *2*, 427–449, 1990.

Dingwell, D. B., D. M. Harris, and C. M. Scarfe, The solubility of H_2O in melts in the system SiO_2-Al_2O_3-Na_2O-K_2O at 1 to 2 kbars, *J. Geol*., *92*, 387–395, 1984.

Dixon, J. E., E. M. Stolper, and J. R. Delaney, Infrared spectroscopic measurements of CO_2 and H_2O in Juan de Fuca Ridge basaltic glasses, *Earth Planet. Sci. Lett*., *90*, 87–104, 1988.

Dixon, J. E., D. A. Clague, and E. M. Stolper, Degassing history of water, sulfur, and carbon in submarine lavas from Kilauea volcano, Hawaii, *J. Geol*., *99*, 371–394, 1991.

Dixon, J. E., E. M. Stolper, and J. R. Holloway, An experimental study of water and carbon dioxide solubilities in mid-ocean ridge basaltic liquids, I, Calibration and solubility models, *J. Petrol*., *36*, 1607–1631, 1995.

Dobson, P. F., S. Epstein, and E. M. Stolper, Hydrogen isotope fractionation between coexisting vapor and silicate glasses and melts at low pressure, *Geochim. Cosmochim. Acta*, *53*, 2723–2730, 1989.

Doremus, R. H., The diffusion of water in fused cilica, in *Reactivity of Solids*, edited by J. W. Mitchell et al., pp. 667–673, John Wiley, New York, 1969.

Doremus, R. H., *Glass Science*, 339 pp., John Wiley, New York, 1994.

Endisch, D., H. Sturm, and F. Rauch, Nuclear reaction analysis of hydrogen at levels below 10 at.ppm, *Nucl. Instrum. Methods Phys. Res*., *Sect. B*, *84*, 380–392, 1994.

Farnan, I., S. C. Kohn, and R. Dupree, A study of the structural role of water in hydrous silica glass using cross-polarisation magic angle spinning NMR, *Geochim. Cosmochim. Acta*, *51*, 2869–2873, 1987.

Fenn, P. M., The nucleation and growth of alkali feldspars from hydrous melts, *Can. Mineral*., *15*, 135–161, 1977.

Fogel, R. A., and M. J. Rutherford, Magmatic volatiles in primitive lunar glasses, I, FTIR and EMPA analyses of Apollo 15 green and yellow glasses and revision of the volatile-assisted fire-fountain theory, *Geochim. Cosmochim. Acta*, *59*, 201–215, 1995.

Friedman, I., and W. Long, Hydration rate of obsidian, *Science*, *191*, 347–352, 1976.

Gilchrist, J., A. N. Thorpe, and F. E. Senftle, Infrared analysis of water in tektites and other glasses, *J. Geophys. Res*., *74*, 1475–1483, 1969.

Goranson, R. W., Silicate-water systems: Phase equilibria in the $NaAlSi_3O_8$-H_2O and $KAlSi_3O_8$-H_2O systems at high temperatures and pressures, *Am. J. Sci*., *35-A*, 71–91, 1938.

Grzechnik, A., and P. F. McMillan, Temperature dependence of the OH absorption in SiO_2 glass and melt to 1975 K, *Am. Mineral*., *83*, 331–338, 1998.

Hamilton, D. L., C. W. Burnham, and E. F. Osborn, The solubility of water and effects of oxygen fugacity and water content on crystallization in mafic magmas, *J. Petrol*., *5*, 21–39, 1964.

Hess, K., and D. B. Dingwell, Viscosities of hydrous leucogranitic melts: A non-Arrhenian model, *Am. Mineral*., *81*, 1297–1300, 1996.

Holtz, F., H. Behrens, D. B. Dingwell, and R. P. Taylor, Water solubility in aluminosilicate melts of haplogranite composition at 2 kbar, *Chem. Geol*., *96*, 289–302, 1992.

Holtz, F., H. Behrens, D. B. Dingwell, and W. Johannes, H_2O solubility in haplogranitic melts: Compositional, pressure, and temperature dependence, *Am. Mineral*., *80*, 94–108, 1995.

Holtz, F., J. Beny, B. O. Mysen, and M. Pichavant, High-temperature Raman spectroscopy of silicate and aluminosilicate hydrous glasses: Implications for water speciation, *Chem. Geol*., *128*, 25–39, 1996.

Ihinger, P. D., An experimental study of the interaction of water with granitic melt, Ph.D. thesis, Calif. Inst. of Technol., Pasadena, 1991.

Ihinger, P. D., R. L. Hervig, and P. F. McMillan, Analytical methods for volatiles in glasses, *Rev. Mineral*., *30*, 67–121, 1994.

Ihinger, P. D., Y. Zhang, and E. M. Stolper, Water speciation in rhyolitic melts, in press, 1999.

Jambon, A., Diffusion of water in a granitic melt: An experimental study, *Year Book*, *Carnegie Inst. Washington*, 352–355, 1979.

Jambon, A., Y. Zhang, and E. M. Stolper, Experimental dehydration of natural obsidian and estimation of D_{H_2O} at low water contents, *Geochim. Cosmochim. Acta*, *56*, 2931–2935, 1992.

Johnson, M. C., A. T. Anderson Jr., and M. J. Rutherford, Preeruptive volatile contents of magmas, *Rev. Mineral.*, *30*, 281–330, 1994.

Kadik, A. A., O. A. Lukanin, Y. B. Lebedev, and E. Y. Korovushkina, Solubility of H_2O and CO_2 in granite and basalt melts at high pressures, *Geochem. Int.*, 1041–1050, 1972.

Karsten, J. L., J. R. Holloway, and J. R. Delaney, Ion microprobe studies of water in silicate melts: Temperature-dependent water diffusion in obsidian, *Earth Planet. Sci. Lett.*, *59*, 420–428, 1982.

Khitarov, N. I., and A. A. Kadik, Water and carbon dioxide in magmatic melts and peculiarities of the melting process, *Contrib. Mineral. Petrol.*, *41*, 205–215, 1973.

Kieffer, S. W., Numerical models of caldera-scale volcanic eruptions on Earth, Venus, and Mars, *Science*, *269*, 1385–1391, 1995.

Kohn, S. C., R. Dupree, and M. E. Smith, A multinuclear magnetic resonance study of the structure of hydrous albite glasses, *Geochim. Cosmochim. Acta*, *53*, 2925–2935, 1989.

Kushiro, I., The system forsterite-diopside-silica with and without water at high pressures, *Am. J. Sci.*, *267-A*, 269–294, 1969.

Lange, R. A., The effect of H_2O, CO_2 and F on the density and viscosity of silicate melts, *Rev. Mineral.*, *30*, 331–369, 1994.

Lapham, K. E., J. R. Holloway, and J. R. Delaney, Diffusion of H_2O and D_2O in obsidian at elevated temperatures and pressures, *J. Non Cryst. Solids*, *67*, 179–191, 1984.

Lesher, C. E., Decoupling of chemical and isotopic exchange during magma mixing, *Nature*, *344*, 235–237, 1990.

Lesher, C. E., Kinetics of Sr and Nd exchange in silicate liquids: Theory, experiments, and applications to uphill diffusion, isotopic equilibrium, and irreversible mixing of magmas, *J. Geophys. Res.*, *99*, 9585–9604, 1994.

Luth, W. C., Granitic rocks, in *The Evolution of the Crystalline Rocks*, edited by D. K. Bailey and R. Macdonald, pp. 335–417, Academic, San Diego, Calif., 1976.

McMillan, P. F., Water solubility and speciation models, *Rev. Mineral.*, *30*, 131–156, 1994.

McMillan, P. F., B. T. Poe, T. R. Stanton, and R. L. Remmele, A Raman spectroscopic study of H/D isotopically substituted hydrous aluminosilicate glasses, *Phys. Chem. Miner.*, *19*, 454–459, 1993.

Moore, G., and I. S. E. Carmichael, The hydrous phase equilibria (to 3 kbar) of an andesite and basaltic andesite from western Mexico: Constraints on water content and conditions of phenocryst growth, *Contrib. Mineral. Petrol.*, *130*, 304–319, 1998.

Moore, G., T. Vennemann, and I. S. E. Carmichael, The solubility of water in natural silicate melts to 2 kilobars, *Geology*, *23*, 1009–1102, 1995.

Moore, G., T. Vennemann, and I. S. E. Carmichael, An empirical model for the solubility of H_2O in magmas to 3 kilobars, *Am. Mineral.*, *83*, 36–42, 1998.

Mysen, B. O., and D. Virgo, Volatiles in silicate melts at high pressure and temperature, 1, Interaction between OH groups and Si^{4+}, Al^{3+}, Ca^{2+}, Na^+ and H^+, *Chem. Geol.*, *57*, 303–331, 1986a.

Mysen, B. O., and D. Virgo, Volatiles in silicate melts at high pressure and temperature, 2, Water in melts along the join $NaAlO_2$-SiO_2 and a comparison of solubility mechanisms of water and fluorine, *Chem. Geol.*, *57*, 333–358, 1986b.

Newman, S., E. M. Stolper, and S. Epstein, Measurement of water in rhyolitic glasses: Calibration of an infrared spectroscopic technique, *Am. Mineral.*, *71*, 1527–1541, 1986.

Newman, S., S. Epstein, and E. M. Stolper, Water, carbon dioxide, and hydrogen isotopes in glasses from the ca. 1340 A.D. eruption of the Mono Craters, California: Constraints on degassing phenomena and initial volatile content, *J. Volcanol. Geotherm. Res.*, *35*, 75–96, 1988.

Nowak, M., and H. Behrens, The speciation of water in haplogranitic glasses and melts determined by in situ near infrared spectroscopy, *Geochim. Cosmochim. Acta*, *59*, 3445–3450, 1995.

Nowak, M., and H. Behrens, An experimental investigation on diffusion of water in haplogranitic melts, *Contrib. Mineral. Petrol.*, *126*, 365–376, 1997.

Ochs, F. A., and R. A. Lange, The partial molar volume, thermal expansivity, and compressibility of H_2O in silicate melts, *Contrib. Mineral. Petrol.*, *129*, 155–165, 1997.

Ochs, F. A., and R. A. Lange, The density of hydrous magmatic liquids, *Science*, *283*, 1314–1317, 1999.

Pandya, N., D. W. Muenow, and S. K. Sharma, The effect of bulk composition on the speciation of water in submarine volcanic glasses, *Geochim. Cosmochim. Acta*, *56*, 1875–1883, 1992.

Papale, P., Modeling of the solubility of a one-component H_2O or CO_2 fluid in silicate liquids, *Contrib. Mineral. Petrol.*, *126*, 237–251, 1997.

Pitzer, K. S., and S. M. Sterner, Equation of state valid continuously from zero to extreme pressures for H_2O and CO_2, *J. Chem. Phys.*, *101*, 3111–3116, 1994.

Qin, Z., I, Diffusive reequilibration of melt inclusions, II, Mathematical modeling of chemical fractionation during mantle melting, Ph.D. thesis, Univ. of Chicago, Chicago, Ill., 1994.

Scholze, H., Zur Frage der Unterscheidung zwischen H_2O-Molekeln und OH-Gruppen in Gläsern und Mineralen, *Naturwissenschaften*, *47*, 226–227, 1960.

Schulze, F., H. Behrens, F. Holtz, J. Roux, and W. Johannes, The influence of H_2O on the viscosity of a haplogranitic melt, *Am. Mineral.*, *81*, 1155–1165, 1996.

Shaw, H. R., Obsidian-H_2O viscosities at 1000 and 2000 bars in the temperature range 700° to 900°C, *J. Geophys. Res.*, *68*, 6337–6343, 1963.

Shaw, H. R., Viscosities of magmatic silicate liquids: An empirical method of prediction, *Am. J. Sci.*, *272*, 870–893, 1972.

Shaw, H. R., Diffusion of H_2O in granitic liquids, I, Experimental data, and II, Mass transfer in magma chambers, in *Geochemical Transport and Kinetics*, edited by A. W. Hofmann et al., pp. 139–170, Carnegie Inst. of Wash., Washington, D. C., 1974.

Shen, A. H., and H. Keppler, Infrared spectroscopy of hydrous silicate melts to 1000°C and 10 kbar: Direct observation of H_2O speciation in a diamond-anvil cell, *Am. Mineral.*, *80*, 1335–1338, 1995.

Shen, A. H., and H. Keppler, Direct observation of complete miscibility in the albite-H_2O system, *Nature*, *385*, 710–712, 1997.

Silver, L., and E. Stolper, A thermodynamic model for hydrous silicate melts, *J. Geol.*, *93*, 161–178, 1985.

Silver, L., and E. Stolper, Water in albitic glasses, *J. Petrol.*, *30*, 667–709, 1989.

Silver, L., P. D. Ihinger, and E. Stolper, The influence of bulk composition on the speciation of water in silicate glasses, *Contrib. Mineral. Petrol.*, *104*, 142–162, 1990.

Skirius, C. M., J. W. Peterson, and J. A. T. Anderson, Homogenizing rhyolitic glass inclusions from the Bishop tuff, *Am. Mineral.*, *75*, 1381–1398, 1990.

Stolper, E. M., Water in silicate glasses: An infrared spectroscopic study, *Contrib. Mineral. Petrol.*, *81*, 1–17, 1982a.

Stolper, E. M., The speciation of water in silicate melts, *Geochim. Cosmochim. Acta*, *46*, 2609–2620, 1982b.

Stolper, E. M., Temperature dependence of the speciation of water in rhyolitic melts and glasses, *Am. Mineral*., *74*, 1247–1257, 1989.

Tuttle, O. F., and N. L. Bowen, Origin of granite in the light of experimental studies in the system $NaAlSi_3O_8$-$KAlSi_3O_8$-SiO_2-H_2O, *Geol. Soc. Am. Mem*., *74*, 1–153, 1958.

van der Laan, S. R., Y. Zhang, A. Kennedy, and P. J. Wylie, Comparison of element and isotope diffusion of K and Ca in multicomponent silicate melts, *Earth Planet. Sci. Lett*., *123*, 155–166, 1994.

Wallace, P. J., A. T. Anderson, and A. M. Davis, Quantification of pre-eruptive exsolved gas contents in silicic magmas, *Nature*, *377*, 612–616, 1995.

Wang, L., Y. Zhang, and E. J. Essene, Diffusion of the hydrous component in pyrope, *Am. Mineral*., *81*, 706–718, 1996.

Wasserburg, G. J., The effects of H_2O in silicate systems, *J. Geol*., *65*, 15–23, 1957.

Wasserburg, G. J., Diffusion of water in silicate melts, *J. Geol*., *96*, 363–367, 1988.

Watson, E. B., Diffusion of cesium ions in H_2O-saturated granitic melt, *Science*, *205*, 1259–1260, 1979.

Watson, E. B., Diffusion in volatile-bearing magmas, *Rev. Mineral*., *30*, 371–411, 1994.

Wilson, L., Relationships between pressure, volatile content and ejecta velocity in three types of volcanic explosions, *J. Volcanol. Geotherm. Res*., *8*, 297–313, 1980.

Wilson, L., R. S. J. Sparks, and G. P. L. Walker, Explosive volcanic eruptions, IV, The control of magma properties and conduit geometry on eruption column behavior, *Geophys. J. R. Astron. Soc*., *63*, 117–148, 1980.

Wyllie, P. J., Magmas and volatile components, *Am. Mineral*., *64*, 469–500, 1979.

Yamashita, S., T. Kitamura, and M. Kusakabe, Infrared spectroscopy of hydrous glasses of arc magma compositions, *Geochem. J*., *31*, 169–174, 1997.

Zhang, Y., Pressure dependence of the speciation of water in rhyolitic glasses (abstract), *Eos Trans. AGU*, *74*(43), Fall Meet. Suppl., 631, 1993.

Zhang, Y., Reaction kinetics, geospeedometry, and relaxation theory, *Earth Planet. Sci. Lett*., *122*, 373–391, 1994.

Zhang, Y., Exsolution enthalpy of water from silicate liquids, *J. Volcanol. Geotherm. Res*., *88*, 201–207, 1999.

Zhang, Y., and H. Behrens, Resolving the controversy between quenched and in situ H_2O speciation in silicate melts and glasses (abstract), *Eos Trans. AGU*, *79*(24), West. Pac. Geophys. Meet. Suppl., W123–W124, 1998a.

Zhang, Y., and H. Behrens, H_2O diffusion in silicate glasses and melts, *Mineral Mag*., *62A*, 1695–1696, 1998b.

Zhang, Y., and E. M. Stolper, Water diffusion in basaltic melts, *Nature*, *351*, 306–309, 1991.

Zhang, Y., E. M. Stolper, and G. J. Wasserburg, Diffusion of water in rhyolitic glasses, *Geochim. Cosmochim. Acta*, *55*, 441–456, 1991a.

Zhang, Y., E. M. Stolper, and G. J. Wasserburg, Diffusion of a multi-species component and its role in the diffusion of water and oxygen in silicates, *Earth Planet. Sci. Lett*., *103*, 228–240, 1991b.

Zhang, Y., E. M. Stolper, and P. D. Ihinger, Kinetics of reaction $H_2O + O = 2OH$ in rhyolitic glasses: Preliminary results, *Am. Mineral*., *80*, 593–612, 1995.

Zhang, Y., R. Belcher, P. D. Ihinger, L. Wang, Z. Xu, and S. Newman, New calibration of infrared measurement of water in rhyolitic glasses, *Geochim. Cosmochim. Acta*, *61*, 3089–3100, 1997a.

Zhang, Y., J. Jenkins, and Z. Xu, Kinetics of the reaction $H_2O + O = 2OH$ in rhyolitic glasses upon cooling: Geospeedometry and comparison with glass transition, *Geochim. Cosmochim. Acta*, *61*, 2167–2173, 1997b.

Zotov, N., and H. Keppler, The influence of water on the structure of hydrous sodium tetrasilicate glasses, *Am. Mineral*., *83*, 823–834, 1998.

Y. Zhang, Department of Geological Sciences, University of Michigan, 2534 C. C. Little Building, 425 E. University Avenue, Ann Arbor, MI 48109-1063. (youxue@umich.edu)